Review

www.the-innovation.org

Milankovitch theory and monsoon

Hai Cheng,[1,2,*] Hanying Li,[1] Lijuan Sha,[1] Ashish Sinha,[1,3] Zhengguo Shi,[1,2] Qiuzhen Yin,[4] Zhengyao Lu,[5] Debo Zhao,[6] Yanjun Cai,[1] Yongyun Hu,[7] Qingzhen Hao,[8] Jun Tian,[9] Gayatri Kathayat,[1] Xiyu Dong,[1] Jingyao Zhao,[1] and Haiwei Zhang[1]

*Correspondence: cheng021@xjtu.edu.cn

Received: August 3, 2022; Accepted: October 13, 2022; Published Online: October 19, 2022; https://doi.org/10.1016/j.xinn.2022.100338

GRAPHICAL ABSTRACT

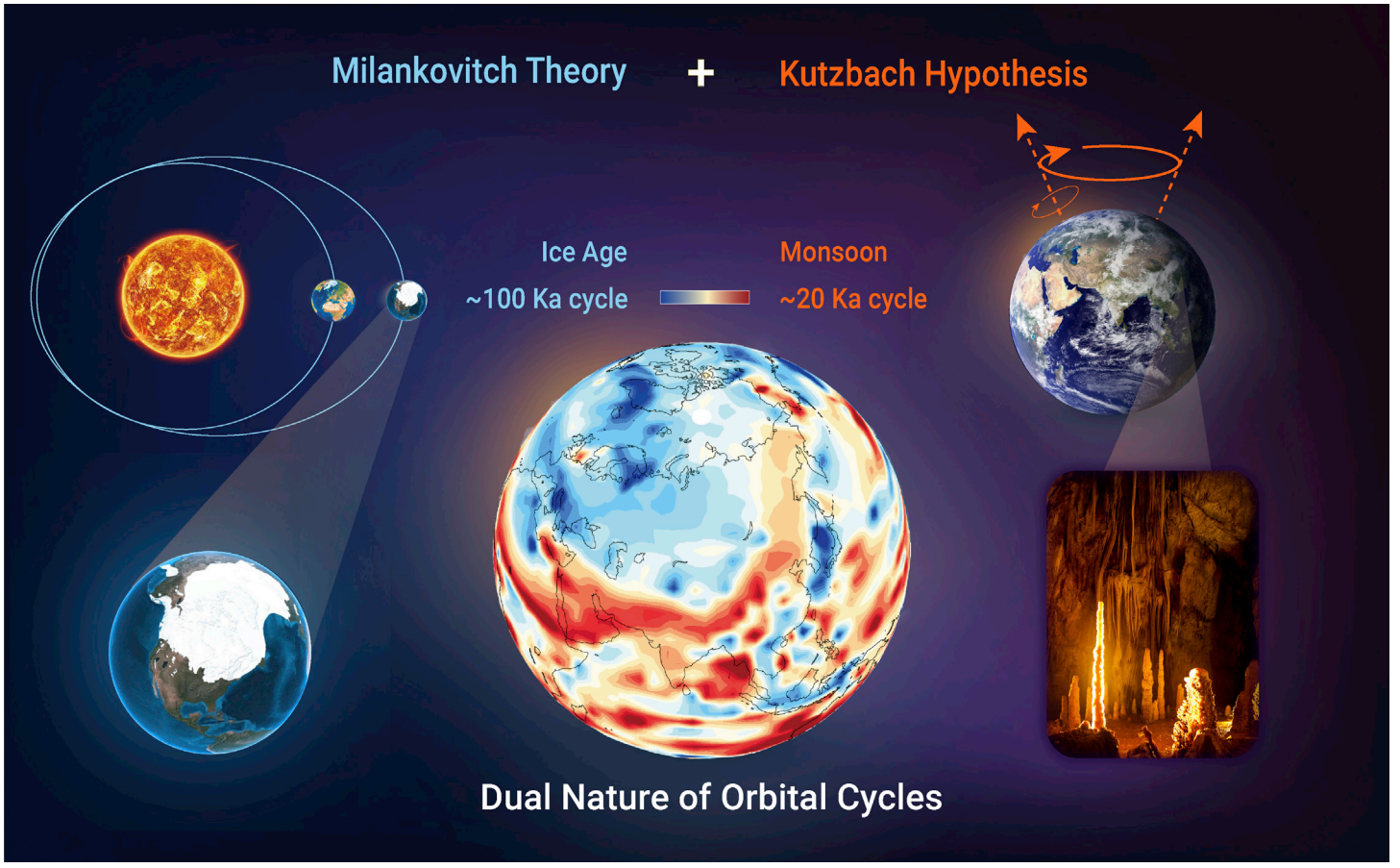

PUBLIC SUMMARY

- Orbital-scale climate variations of Earth are dictated by ice sheet and monsoon
- Views of “monsoon system science” reinforce the Kutzbach monsoon hypothesis
- A unified Milankovitch-Kutzbach hypothesis better explains the orbital dual nature

Review

Milankovitch theory and monsoon

Hai Cheng,[1,2,*] Hanying Li,[1] Lijuan Sha,[1] Ashish Sinha,[1,3] Zhengguo Shi,[1,2] Qiuzhen Yin,[4] Zhengyao Lu,[5] Debo Zhao,[6] Yanjun Cai,[1] Yongyun Hu,[7] Qingzhen Hao,[8] Jun Tian,[9] Gayatri Kathayat,[1] Xiyu Dong,[1] Jingyao Zhao,[1] and Haiwei Zhang[1]

[1]Institute of Global Environmental Change, Xi'an Jiaotong University, Xi'an 710049, China
[2]State Key Laboratory of Loess and Quaternary Geology, Institute of Earth Environment, Chinese Academy of Sciences, Xi'an 710061, China
[3]Department of Earth Sciences, California State University, Dominguez Hills, Carson, CA 90747, USA
[4]Georges Lemaître Center for Earth and Climate Research, Earth and Life Institute, Université Catholique de Louvain, 1348 Louvain-la-Neuve, Belgium
[5]Department of Physical Geography and Ecosystem Science, Lund University, Sölvegatan 12, 22362 Lund, Sweden
[6]Key Laboratory of Marine Geology and Environment, Institute of Oceanology, Chinese Academy of Sciences, Qingdao 266071, China
[7]Department of Atmospheric and Oceanic Sciences, School of Physics, Peking University, Beijing 100871, China
[8]Key Laboratory of Cenozoic Geology and Environment, Institute of Geology and Geophysics, Chinese Academy of Sciences, Beijing 100029, China
[9]State Key Laboratory of Marine Geology, Tongji University, Shanghai 200092, China
*Correspondence: cheng021@xjtu.edu.cn

Received: August 3, 2022; Accepted: October 13, 2022; Published Online: October 19, 2022; https://doi.org/10.1016/j.xinn.2022.100338

Citation: Cheng H., Li H., Sha L., et al., (2022). Milankovitch theory and monsoon. The Innovation **3(6)**, 100338.

The widely accepted "Milankovitch theory" explains insolation-induced waxing and waning of the ice sheets and their effect on the global climate on orbital timescales. In the past half century, however, the theory has often come under scrutiny, especially regarding its "100-ka problem." Another drawback, but the one that has received less attention, is the "monsoon problem," which pertains to the exclusion of monsoon dynamics in classic Milankovitch theory even though the monsoon prevails over the vast low-latitude (~30° N to ~30° S) region that covers half of the Earth's surface and receives the bulk of solar radiation. In this review, we discuss the major issues with the current form of Milankovitch theory and the progress made at the research forefront. We suggest shifting the emphasis from the ultimate outcomes of the ice volume to the causal relationship between changes in northern high-latitude insolation and ice age termination events (or ice sheet melting rate) to help reconcile the classic "100-ka problem." We discuss the discrepancies associated with the characterization of monsoon dynamics, particularly the so-called "sea-land precession-phase paradox" and the "Chinese 100-ka problem." We suggest that many of these discrepancies are superficial and can be resolved by applying a holistic "monsoon system science" approach. Finally, we propose blending the conventional Kutzbach orbital monsoon hypothesis, which calls for summer insolation forcing of monsoons, with Milankovitch theory to formulate a combined "Milankovitch-Kutzbach hypothesis" that can potentially explain the dual nature of orbital hydrodynamics of the ice sheet and monsoon systems, as well as their interplays and respective relationships with the northern high-latitude insolation and inter-tropical insolation differential.

INTRODUCTION

One of the foremost advances in Earth science occurred in the 20th century with the revival of the theory of orbital forcing of the late quaternary glacial cycles, known as the Milankovitch theory.[1] The theory postulates that changes in caloric summer half-year insolation (or Northern hemisphere summer insolation [NHSI]) at ~65° N latitude, a region critical for initiation of glaciers, in response to cyclical changes in the Earth's orbital geometry (eccentricity, obliquity, and precession) drive the rhythmic growth and retreat of the Northern hemisphere (NH) ice sheet (the *sensu stricto* theory). The waxing and waning of the ice sheet, in turn, are hypothesized to incite ancillary changes in other parts of the global climate system via various forcing and response/feedback mechanisms (the *sensu lato* hypothesis).

In its early years, Milankovitch theory was not widely accepted because of a lack of corroborating geological evidence. It was not until publication of seminal work[2] that the Milankovitch theory acquired widespread acceptance and became the canonical theory of Earth's orbital-scale climate change. The high-resolution oxygen isotope ($\delta^{18}O$) time series of planktonic foraminifera was the first record of its kind that revealed variations in the global ice volume over the past ~450 kiloannums (ka).[2] The record indicated that variations in the global ice volume occurred in a sawtooth pattern characterized by an ~100-ka quasi-cycle superimposed by shorter quasi-cycles of ~41, ~23, and ~19 ka, as predicted by the Milankovitch theory. These periodicities were also found independently in long-term variations of eccentricity, obliquity, and climatic precession using an analytical solution of the planetary system.[3] In particular, the existence of double precession peaks (the so-called "Berger cycles" of ~23 and ~19 ka) in the $\delta^{18}O$ records and astronomical solutions become strong validation of the astronomical theory. Subsequent developments of the marine records presented evidence of the ~100-ka cycle of glaciation, supporting in part the dominant role of high-latitude processes in global climate variations.[4–7] However, to date, several unsolved problems associated with the theory remain, such as the "100-ka problem";[2] namely, that the orbital eccentricity (~100-ka cycle) contributes much less to isolation change than precession (~20-ka cycle) and obliquity (~40-ka cycle), and yet, the most significant variation in the ice volume over the past ~800 ka is the ~100-ka glacial-interglacial cycle, similar to the orbital eccentricity cycle.

Despite various problems, the Milankovitch theory has now become accepted wisdom, and it has led to development of an interpretative framework in which the high-latitude glaciation processes takes central stage, and the low-latitude large-scale tropical monsoon systems[8–10] are essentially excluded. The exclusion of the latter in the "conventional" Milankovitch theory presents another problem, the "monsoon problem," which is described by Imbrie et al.[6] as follows: "Because our focus is on the process of glaciation, we exclude low-latitude sites where previous work has shown that climate history is dominated by changes in the monsoon circulation. In fact, this strategy may well exclude consideration of low-latitude processes that could be important in changing the concentrations of methane and water vapor in the atmosphere".

About half of the Earth's surface lies between ~30° N and ~30° S, where a monsoon climate prevails. The vast low-latitude monsoon and ice sheet-dominated high-latitude climate regimes constitute the two major planetary-scale climatic systems with complex interactions.[11,12] Theoretical and proxy considerations indicate that two distinct orbital insolation forcings are prominent, with low-latitude insolation forcing dominating the monsoon variations with strong ~20-ka precession cycles[8,13–18] and NH high-latitude summer insolation forcing driving ice sheet variations with dominant ~100-ka cycles.[2,19] Therefore, a comprehensive orbital theory would ideally explain not only high-latitude ice sheets but also the embedded low-latitude monsoons as well as the interplay between high- and low-latitude hydroclimates in the context of the distinctive dual insolation forcings. The Kutzbach orbital monsoon hypothesis (namely, that tropical monsoons vary in response to summer insolation)[8,20] remains in dispute.[21,22] The central issues here involve the spatiotemporal nature of the low-latitude monsoon hydroclimate on an orbital scale, the underlying dynamics, the relation to insolation forcing, as well as key interplay between the monsoon and the ice sheet. A thorough understanding of these issues is prerequisite to formulate a more comprehensive form of the orbital theory of climate.

Breakthroughs in the U/Th dating technique[23] in the past decade have propelled speleothems to the forefront of paleoclimatology. The speleothem records of past climate are now considered the strong fourth leg of the paleoclimate "tetrarchate,"[20,24,25] after the three main orbital-scale paleoclimate archives: the marine, ice core, and loess records. One of the key advantages of speleothem records is their absolute and precise chronology in contrast to the essentially orbitally tuned chronology of marine, ice core, and loess records. In this review, we do not attempt to resolve all outstanding issues surrounding the Milankovitch theory;[26] instead, we highlight the millennial-scale variations over the last several glacial-interglacial cycles, inferred from absolutely dated speleothem records,

including ice age terminations, to analyze the relationship between insolation and Earth's hydroclimate responses, which may help to reconcile the "100-ka problem." We then assess the dominant orbital rhythm of precession variability across the low-latitude monsoon regime, especially the phases and spatial variances over multiple ice age cycles as informed by the speleothem and marine records. We also examine the critical hypotheses of climate responses, such as the "early response" and "late response," to summer insolation at the precession band[6,13] and high- and low-latitude climate interplay via absolutely dated speleothem records from ice sheet-proximal regions and remote low-latitude tropical monsoon regimes. We show that the crucial discrepancies surrounding the Kutzbach orbital monsoon hypothesis might be superficial and may be reconciled within the framework of "monsoon system science." Last, we build on the key aspects of the Milankovitch theory[1,2] and Kutzbach orbital monsoon hypothesis[8,20] for high- and low-latitude hydroclimate variations on orbital scales; together with results from previous studies of speleothems, ice cores, and loess and marine sediments, we sketch a primary orbital climate hypothesis that also comprises key elements of monsoonal climate variability at orbital scale and the major climate dynamics.

THE "100-KA PROBLEM" AND MILLENNIAL-SCALE EVENTS

The so-called "100-ka problem" is a classic issue that has been associated with the Milankovitch theory from the very beginning.[2] Several competing hypotheses have been put forth to address this problem. The significant ~100-ka periodicity of glaciation has been linked to the Earth's eccentricity cycle,[27,28] 2–3 obliquity cycles,[29–31] a combination of obliquity and precession,[16,32–34] and an average of 4–5 discrete precession cycles.[16,35,36] Other hypotheses call for interactions involving internal oscillations in the Earth system,[28,37–39] particularly dynamics of global ice volume and atmosphere CO_2 changes, invoking non-linearities to amplify the rather modest changes in insolation forcing.[2,19,40–43] The observation that the 100-ka cycles in the geological records become strong at a time when the eccentricity is weak suggests that the 100-ka cycles cannot come from the eccentricity but rather from the non-linear response (especially from the ice sheet)[44] to the variations of climatic precession of 23- and 19-ka periods.[45]

Theoretically, the apparent mismatch between the benthic $\delta^{18}O$ records (or global ice volume) and insolation (i.e., the 100-ka problem) suggests the presence of some type of internal feedback mechanism of the Earth. Based on simple physics, it has been proposed that the rate of change, rather than absolute global ice volume per se, should be dynamically more important to retain a direct anti-correlation with summertime insolation over northern high latitudes.[46,47] The correlation of 65° N summer insolation with the rate of ice volume (or sea level) change[7,48] is more significant than with ice volume itself (Figure 1A). However, a potential weakness of this correlation is that the chronologies of ice volume and sea level are ultimately "tuned" to insolation, leading to a "circular logic." To avoid this drawback, an absolutely dated monsoon record over the past ~640 ka, together with its correlations with other hydroclimate records,[50,51] was utilized to analyze the Milankovitch theory in terms of the relationship between insolation variation and ice age termination events.[16] It was found that all seven conventional terminations over the past ~640 ka occurred during the rising limbs of NHSI separated by 4, 5, 5, 4, 5, and 5 precession or ~2, 3, 2, 2, 3, and 3 obliquity cycles with durations of 93, 105, 92, 92, 113, and 115 ka, respectively.[16] Two "extra terminations", termination IIIa (T-IIIa),[29] which occurred about one precession cycle after T-III (between MIS 7.4 and 7.3), and T-VIIa, which occurred about two precession cycles after T-VII (between MIS 15.2 and 15.1) (Figure 1), exhibit a pattern similar to the seven conventional terminations with a comparable amplitude of marine benthic $\delta^{18}O$ or sea level changes.[7,48] Under this circumstance, each of the nine terminations is separated from adjacent terminations by an integral number of precession cycles, suggesting precession pacing terminations. All nine terminations took place when the obliquity was substantially higher than the average, suggesting its causal role as well.[29,30,32,34]

The notion that the ~100-ka cycle encompasses an average of 4–5 discrete precession cycles or 2–3 discrete obliquity cycles invokes missed "beats" between major terminations. The underlying mechanism may involve Earth's internal nonlinear responses/feedback (e.g., ice sheet dynamics, CO_2 changes, and ocean circulation reorganizations). One piece of evidence is that the middle Pleistocene transition (MPT) from the "40-ka world" to the "100-ka world" occurred at ~800–1000 ka BP (before present, where present = 1950 CE) without associated considerable shifts in astronomical parameters,[49,52] implying that internal forcing, rather than external insolation, changed the tempo of the Earth system response to the external orbital forcing. On the other hand, several studies have focused on the cause of skipped precession and/or obliquity beats between major terminations.[29,33,35] Subsequent studies found that small-scale millennial events with a nature similar to the major termination events occurred proximate to times when large termination beats were missed.[16,51] Therefore, these millennial events have been named "low-amplitude version of terminations,"[53] "failed terminations,"[54] or "unfinished terminations."[55] Explanations for full- versus small-scale terminations have also focused on interplay and feedback among factors internal to the Earth's climate system, such as ice sheet dynamics and atmospheric CO_2 in the context of certain orbital forcing states.[33,56–59]

Conventional ice age termination events and other millennial-scale events have been shown to be essentially similar except for their amplitudes.[16,25,50,51] To analyze the relationship between insolation and millennial events, time series of millennial-scale variations were obtained by removing the orbital insolation signal from the Asian Monsoon (AM) speleothem $\delta^{18}O$ record ($\Delta\delta^{18}O$) and the long-term trend from the Antarctic ice core δD (temperature proxy) record (ΔδD) (Figure 1B and 1C).[16] These detrended records largely characterize millennial-scale climate variations involving both conventional ice age terminations and low-amplitude versions of termination events. The millennial-scale climate variations deciphered from detrended AM ($\Delta\delta^{18}O$) and Antarctic temperature (ΔδD) records show prominent precession and obliquity cycles (Figures 1E and 1F),[16] similar to the change rate of ice volume (Figure 1D). The phase analyses indicate that large change rates of ice volume (or ice sheet melting) and significant millennial events, including conventional terminations, tend to occur at the precession minima (P_{min}; around NH June insolation maxima)[16,60] under the high-obliquity state, resulting in weak AM and Antarctic warming, a manifestation of the "bipolar seesaw" pattern.[61] A recent model simulation also shows that a precession-controlled increase in low-latitude boreal summer insolation around P_{min} raises the temperature over the tropical Atlantic, which weakens trade winds and reduces Atlantic water vapor, resulting in a decrease in Atlantic sea surface salinity (SSS) and Atlantic meridional overturning circulation (AMOC) slowdown.[62] These observations and simulations indicate that insolation, as a possible ice age termination trigger, might never really miss a beat at precession/obliquity pacing. What was missed was the same amplitude of Earth's internal response/feedback in terms of the ice sheet/CO_2 changes. In this interpretative framework, a northern high-latitude summer insolation increase would accelerate ice sheet melting (Figure 1A)[46,47] and trigger millennial events (Figure 1B) and associated atmospheric CO_2 variations,[50,51] leading to the observed different amplitude of terminations in the proxy records.[16] Therefore, the longstanding and most critical problem associated with the Milankovitch theory, the "100-ka problem," seems to be not vital any longer, provided that the central concern lies in high-latitude NHSI driving the ice sheet change mostly at precession/obliquity pacing rather than the ultimate outcomes that are largely dependent on Earth's internal nonlinear responses/feedback, which are not particularly explained by the theory.[46,47]

LOW-LATITUDE MONSOON

The monsoon climate prevails over about half of the Earth's surface between ~30° N and ~30° S (Figure 2).[17,18] The amount of solar energy received in the region is an order of magnitude more than that received above 65° N. Until now, the Milankovitch theory essentially does not involve monsoon dynamics,[6] called here the "monsoon problem." This is a critical limitation of the current orbital theory of climate, which focuses mainly on the Earth's climate system at high latitudes. A more encompassing version of the orbital theory should include, rather than exclude, the global monsoon system. To involve the monsoon in an orbital theory, a systematic understanding of monsoon dynamics on orbital scale is essential.

The monsoon is nowadays recognized as a global-scale, three-dimensional atmospheric circulation characterized by seasonal reversal in surface wind/rainfall and migration of the inter-tropical convergence zone (ITCZ). The latter is linked closely to the reversal in temperature gradients between continents and ocean and/or the NH and Southern hemisphere (SH) in response to the annual solar radiation cycle.[64,66] Similarly, in paleoclimate world, the global monsoon also defines the major hydroclimate mode across a vast portion of the Earth's tropics-subtropics on a wide range of timescales (Figure 2).[15,17,18,67,68] The major monsoon subsystems in the world include the AM, North African monsoon (NAFM), and North American monsoon (NAM) in NH low to mid-latitudes and

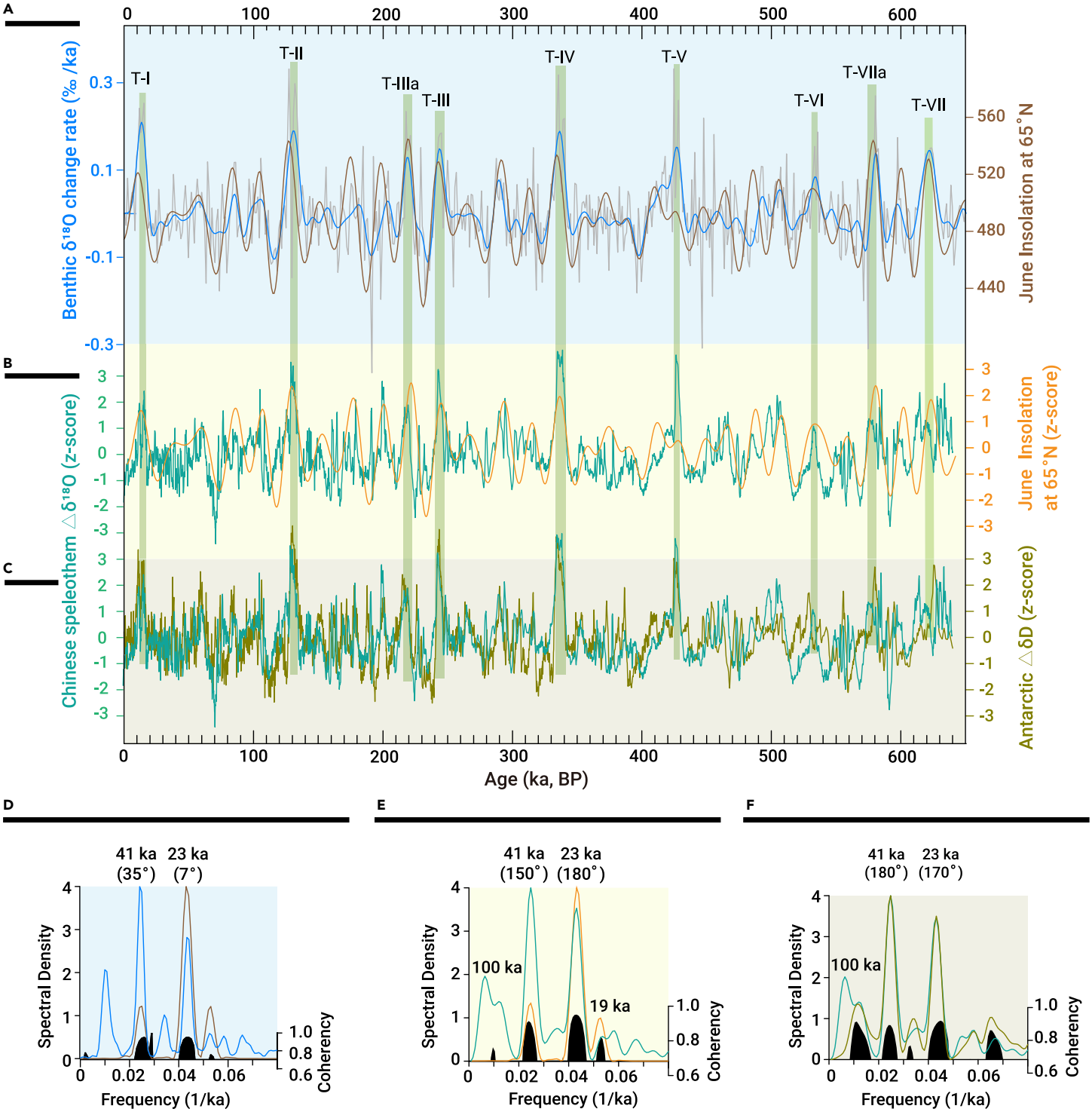

Figure 1. Relationships between the benthic $\delta^{18}O$ change rate, suborbital-scale AM and Antarctic temperature variations, and insolation (A) Benthic $\delta^{18}O$ (LR04)[7] change rate (gray) and its 10-ka low pass (blue). June insolation at 65°N is shown by the brown curve.[49] The correlation between the 10-ka low pass of the benthic $\delta^{18}O$ record and June insolation at 65° N is significant, with a correlation coefficient of 0.59. (B) Suborbital AM variation ($\Delta\delta^{18}O$) (green curve in *Z* score, detrended from the composite $\delta^{18}O$ record by subtracting 21 July insolation at 65° N from the composite AM $\delta^{18}O$ record)[16] and June insolation at 65° N (orange curve in *Z* score).[49] (C) AM $\Delta\delta^{18}O$ (green curve in *Z* score)[16] and Antarctic suborbital temperature variation ($\Delta\delta D$) (olive curve in *Z* score; detrended from the δD record).[16] (D) Spectral analysis results of June insolation at 65° N (brown) and the benthic $\delta^{18}O$ change rate (blue)[7] and their coherence spectra (black). (E) Spectral analysis results of 21 June insolation at 65° N (orange)[49] and AM $\Delta\delta^{18}O$ records (green)[16] and their coherence spectra (black). (F) Spectral analysis results of AM $\Delta\delta^{18}O$ records (green)[16] and detrended Antarctic $\Delta\delta D$ records (olive) and their coherence spectra (black). Coherence spectra are at an 80% confidence level. Numbers in parentheses show phase differences in degrees between two spectra at precession (~23- and 19-ka) and obliquity (~41-ka) bands. Precession and obliquity periodicities of ~23 and ~41 ka are significant in all four datasets (the benthic $\delta^{18}O$ change rate, June insolation at 65° N, AM $\Delta\delta^{18}O$, and Antarctic $\Delta\delta D$). Cross-spectrum analyses elucidate a phase coherency (broadly in phase) at precession and obliquity bands between the benthic $\delta^{18}O$ and the June insolation, the AM $\Delta\delta^{18}O$ and the June insolation, and the Antarctic $\Delta\delta D$ and June insolation. These observations impl that the high-latitude insolation-induced ice sheet melting triggered the millennial-scale events in the North Atlantic mostly at the precession/obliquity pacing, which, in turn resulted in weak AM events and Antarctic warming with approximate in-phase precession/obliquity periodicities. Adapted from Cheng et al.[16,25]

Indonesian-Australian monsoon (IAM), South African monsoon (SAFM), and South American monsoon (SAM) in SH low latitudes (Figure 2).[64] Although each of these regional monsoon systems has specific characteristics, all are co-ordinated largely by the annual cycle of solar radiation, thus displaying a similar fashion (Figure 2). Comparably, on the orbital scale, the insolation variations dominated by precession also appear to coordinate variations of monsoon

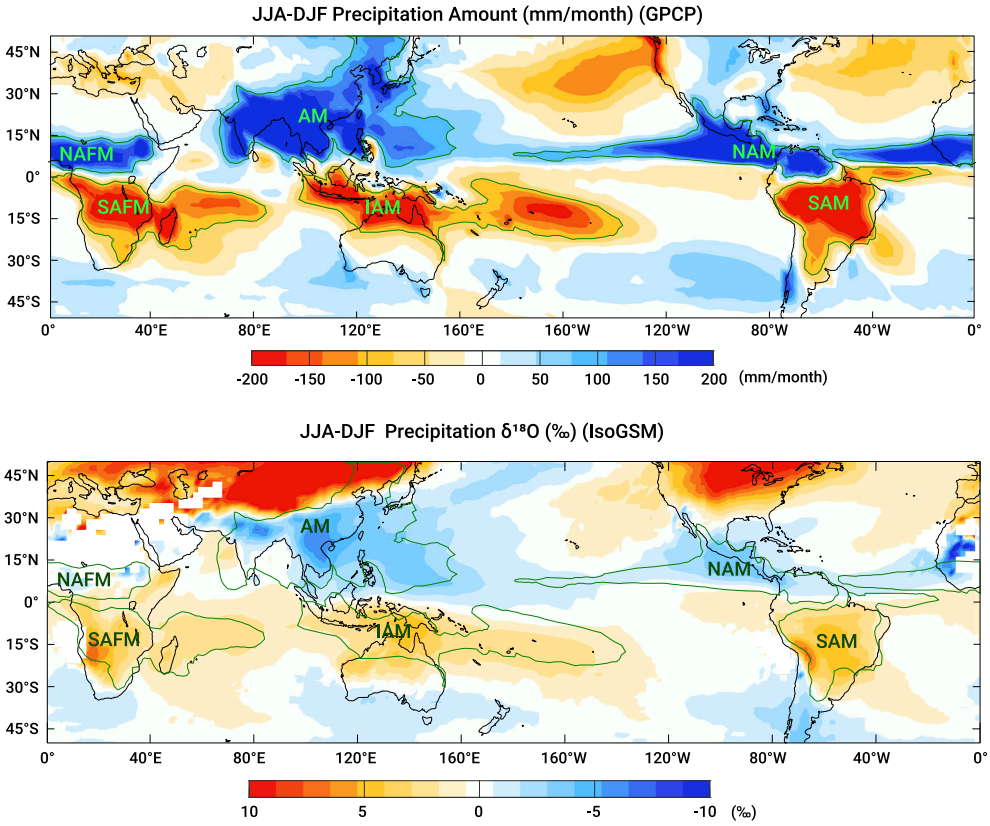

Figure 2. Modern monsoon systems Upper Panel: Shown is the precipitation difference (1979–2016) between JJA and DJF from Global Precipitation Climatology Project (GPCP) version 2.3.[63] The green lines show ~80 (or -80) mm/month contours, which are used to approximately indicate spatial extents of six sub-monsoon systems: the Asian monsoon (AM), North African monsoon (NAFM) and North American monsoon (NAM), Indonesian-Australian monsoon (IAM), South African monsoon (SAFM), and South American monsoon (SAM) systems.[64] Lower Panel: The precipitation $\delta^{18}O$ difference between the JJA and DJF was simulated by IsoGSM2[65] (1979–2016). Boreal and austral summer monsoon rainfalls show more negative $\delta^{18}O$ values than their winter precipitations.

changes as the major forcing, although the global ice volume and greenhouse gases also influence this as internal forcing/feedback to some extent, especially in the mean annual precipitation and temperature in the monsoon regime.[69,70] In terms of hydrological cycles, vapor-water transition constitutes the essence of the low-latitude monsoon regime, with a dominant precession cycle on orbital scale, in contrast to the liquid-solid transition prevailing in the high-latitude regime, with dominant ~100-ka glacial-interglacial cycles in the Late Quaternary.[16,67,71–73] In fact, the monsoon has long been theoretically demonstrated to be primarily driven by tropical solar insolation[8] with dominated precession cycles. If so, then the orbital-scale expression of monsoons ought to be dominated by precession cycles accordingly. A significant body of observational data[16,74] and model simulations[14,71,75–77] supports this hypothesis. However, the precession phases of monsoon orbital variations are apparently more complex, constituting one of the fundamental paradoxes, as discussed below.

Monsoon variations at the precession band

From the astronomical point of view, precession variations overwhelmingly dominate insolation changes over the tropical-subtropical monsoon regime.[49,52] The monsoon variability has been shown to be a magnitude more sensitive to summer insolation forcing than to glacial-interglacial boundary conditions from observational[15–17,74] and theoretical considerations,[13,18,75,78,79] manifesting a primary rhythm of precession cycles. This is largely because the low-latitude monsoon circulation and associated precipitation respond sensitively to the thermal gradient resulting from the difference between thermal properties of continents and oceans, which is amplified (weakened) by larger (smaller) seasonal solar radiation extremes induced by precessional changes.[78] The Earth's orbital precession affects the seasonal distribution of solar radiation, resulting in an increase in northern tropical-subtropical summer insolation that is balanced by a decrease in southern tropical-subtropical summer insolation and vice versa. Therefore, it is also expected that monsoons should be registered as an inter-hemispherically anti-phased relationship at the precession band, which has been substantiated by observations of the precessional see-sawing between speleothem records from the AM system in the NH[16] and the SAM system in the SH,[74,80] similar to the seasonal variability between the two monsoon systems (Figures 2 and 3). Although obliquity and eccentricity also contribute to insolation variations, they are generally less important, at least for daily and seasonal mean insolation, especially in the low-latitude monsoon regime.[49,52] Monsoons are typically characterized by the moist summer circulations that provide most of the annual rainfall to terrestrial lands in the tropics and subtropics. Dynamically, the sensitivity of the monsoonal hydrological cycle to orbital parameter changes is also significantly larger in summer than in winter.[78] Therefore, unless otherwise specified, we highlight the summer monsoon variations in the following discussions.

Ruddiman[13,81] proposed two types of hydroclimate responses to summer insolation changes at the precession band. (1) The "late response": NH summer (or June 21) insolation forces a significantly lagged (~5-ka) ice sheet response and transfers to proximal regions, which is one of the key aspects of the Milankovitch theory. (2) The "early response": hydroclimate changes in regions remote to the ice sheet, such as monsoons, respond directly to summer insolation without significant lags. Theoretically, the monsoon precessional variations are presumably sensitive to changes in low-latitude insolation and, thus, most likely to lead the ice sheet change. However, the relationship of precession phases between the ice volume and monsoon variations lacks vigorous testing. This is because the ice volume change at the precession band was orbitally tuned with an assumed lag of ~5 ka to NH June 21 insolation,[2,4,6] which lacks independent verification from precisely dated geological archives. Of particular interest are the recent speleothem records reconstructed from Buckeye Creek Cave (BCC) in east-central North America at the southern fringe of the maximum North American ice sheet,[82] which may potentially provide a test for the longstanding issue of precession phase lag, because the climate variability at the ice sheet-proximal regions is presumably sensitive to the ice sheet extent signals, which influence the proximal regions via atmospheric/oceanic processes.[6,13] The phase analysis shows that the BCC $\delta^{18}O$ record indeed lags the NH June 21 insolation (NHSI) at the precession band by ~5 ka (in phase with September insolation) (Figure 4), consistent with the modeling results[83] and supporting the conventional assumption of an ~5 ka lag of the ice sheet change relative to NH June insolation at the precession band. This lagged response of the ice sheet agrees well with the "late response" scenario. On the other hand, several absolutely dated speleothem $\delta^{18}O$ records from the AM, Asian Westerly (AW), and SAM systems suggest prominent precession pacing of mid- to low-latitude hydroclimate.[16,74,80,84–89] At the precession band, these records are essentially in phase with ~July 21 insolation (i.e., AM-AW records)[16,89,90] and ~January 21 insolation (i.e., SAM records)[74,80] (Figures 3 and 4), consistent with model simulations[14,91] and the "early response" hypothesis.[13]

The apparent ~2- to 3-ka lag of the AM (SAM) to June 21 (December 21) insolation in the speleothem records may be explained by millennial-scale weak (strong) monsoon events with durations comparable with the lag that often occurred at the rising (falling) limbs of insolation in the NH (SH) (Figure 3).[16,51,92,93] Another interpretation underlines the ice volume forcing, which lags the June 21 insolation by ~5 ka at the precession band and, thus, could theoretically produce the observed lag of ~2–3 ka in combination with the in-phase insolation forcing.[94–96] However, when we take monsoon variations in SH into consideration,

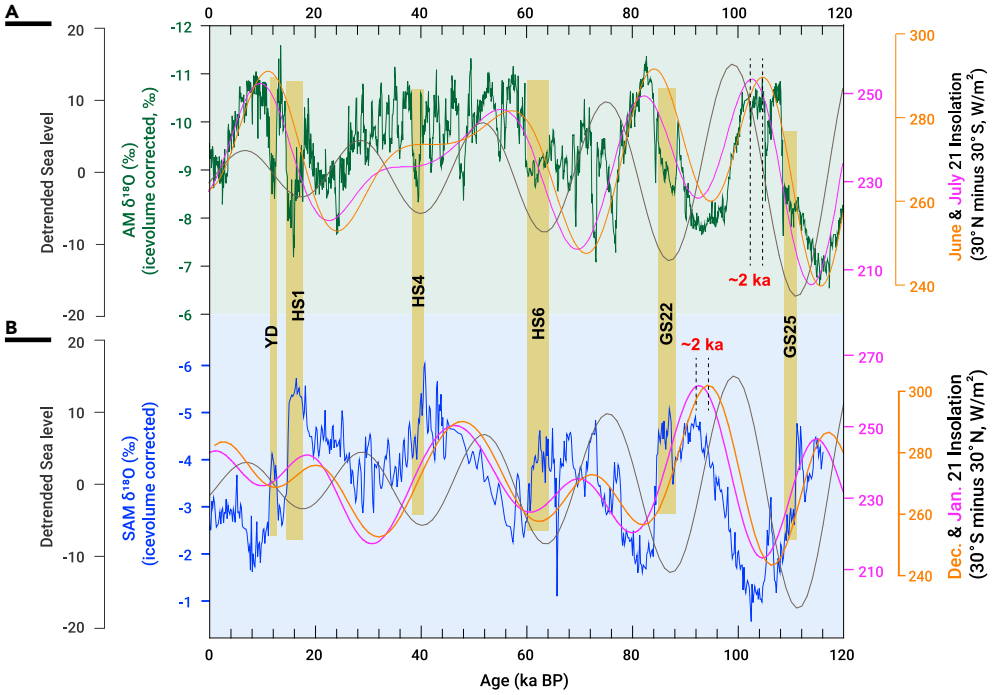

Figure 3. Comparison of AM and SAM speleothem $\delta^{18}O$ records with insolation and ice volume changes at the precession band (A) AM speleothem $\delta^{18}O$ record (green, ice volume corrected),[16] 30° N–30° S June 21 (orange) and July 21 (pink) insolation[49] and the sea level variation at the precession band (dark gray) (filtered using Gaussian filtering at the precession band; frequency, 0.0435; bandwidth, 0.01).[48] (B) SAM speleothem $\delta^{18}O$ record (blue, ice volume corrected),[74] 30° S–30° N December 21 (orange) and January 21 (pink) insolation,[49] and filtered sea level variation at the precession band (dark gray).[48] The major millennial-scale event/stadials (Younger Dryas [YD]; HS1, HS4, and HS6; and Greenland stadials 22 and 25) occurred at the rising (falling) limbs of insolation in the NH (SH), which have a similar duration compared with the 2- to 3-ka lag of ASM (SAM) to the June 21 (December 21) insolation at the precession band.

the ice volume hypothesis becomes rather complicated. Although ice volume forcing seems to be able to account for the AM lag, it would be difficult to explain the same temporal lag of the SAM, unless there exists a completely different mechanism in the SH regarding the ice sheet's influence on monsoons (Figure 3). Provided that the above interpretation is sound, the ice volume effect on low-latitude monsoons would be somewhat small at the precession band.

Based on transient simulations, Kutzbach et al.[14] also found an ~2- to 3-ka lag of the monsoon precipitation response to the orbital summer insolation forcing at the precession band so that, on average, the monsoon July (January) precipitation maxima and JJA (DJF) precipitation maxima have high coherence. They suggested that the lag was well within the phase limit constrained by the control factors of monsoon precipitation— both thermal dynamics (land/ocean temperature contrast and land sea-level pressure minima) and hydrological dynamics relating to the sea surface temperature (SST), evaporation from the ocean, and landward transport of water vapor.[14] Because changes in atmospheric greenhouse gases, atmospheric dust loading, ice volume, and sea level were not considered in this model simulation, the 2- to 3-ka lag of the monsoon response apparently could be explained by orbital insolation forcing alone without the necessity to involve the ice volume.

Another hypothesis emphasizes that monsoon is largely driven by intertropical insolation differences (or sensible heat difference) or the resultant pressure gradient between approximately the Tropics of Cancer (~23° N) and Capricorn (~23° S), the summer inter-tropical insolation gradient (SITIG).[97] This idea can account, to some extent, for the SH effect on the AM but differs mechanistically from another longstanding hypothesis, that the AM is driven largely by the latent heat originating from the Southern Indian Ocean, which reaches the maxima on the orbital scale near the time of the minima of SH winter insolation (~11-ka lag to NH June 21 insolation).[94,95] Similarly, several studies also considered the interhemispheric insolation differential (e.g., the insolation differential between 30° N and 30° S) as the forcing of the AM.[93,98,99] In fact, the June 21 insolation differential between 30° N and 30° S (or between 23° N and 23° S) and the insolation at the high latitude of 65° N are virtually identical in terms of their phase, net range, and pattern of variations. However, their influence on Earth's hydroclimate systems is quite different. Mechanistically, June 21 insolation at NH high latitude is commonly considered the critical forcing driving changes in ice sheet extent (Milankovitch theory), whereas the June 21 (December 21) insolation differential between the interhemispheric tropics propels NH (SH) monsoon variations on the orbital scale. Although it is conventional wisdom that NH (SH) tropical summer insolation drives NH (SH) monsoon on the orbital scale,[8] physically, the interhemispheric differential in tropical insolation (or SITIG) appears to be a more integrated forcing of monsoons. This is because the insolation difference involves "pull" and "push" forcings from two hemispheres that propel monsoon changes.[93,97–102] One line of evidence lies in the variation of the AM across the ~60- to 25-ka BP interval in the last glacial, which manifests as a slightly declining trend akin to the insolation differentials (Figure 4B), rather than local NH tropical summer insolation, which has a distinct precessional insolation minimum around ~45 ka BP in the interval.[98] Notably, however, the role of the SH in driving the AM was apparently strong during glacials and weak during interglacials.[101–103] In the aforementioned interpretative framework, the monsoon early response and the ice sheet late response suggest that the *sensu lato* Milankovitch theory (or the ice volume forcing drives Earth's hydrological changes) may not be perfectly suitable in the monsoon world at the precession band,[13] though the *sensu stricto* Milankovitch theory retains validity.

Phases of monsoon variations at the precession band

The orbital forcing-induced hydroclimate changes in the monsoon regime show extensive precession variability. However, a closer look suggests that the precession phases of monsoonal hydroclimate variations are quite complex, depending on the regional dynamic in different parts of the monsoon system. In the current interpretative framework,[25,93] when the modern AM becomes stronger with the annual increase of land-sea thermal contrast from spring to summer, the spatial scale of the summer monsoon circulation expands progressively, and more remote moisture is transported farther northwest into the Asian continent. The summer monsoon fringe extends northward, and overall summer monsoon precipitation increases over the continent, specifically over the northwestern fringe regions of the AM system, whereas the overall precipitation $\delta^{18}O$ becomes more negative in most continental regions (Figure 2). These modern observations[25,104,105] provide an approximate analog (similar seasonality dynamics) to the AM intensification process from low to high NHSI conditions or from the precession maximum (P_{max}) to the P_{min} state and vice versa. These processes are now demonstrated consistently in many modeling results (Figure 5).[14,71,75–77,113–120] Even over the arid regions (e.g., the Tarim Basin), the precipitation seems to follow these insolation-induced AM changes as well.[87] A large body of paleo-monsoon records has also shown that the AM changes from P_{max} to P_{min} (low to high NHSI) manifest an overall increased summer rainfall and decreased rainfall $\delta^{18}O$ in most parts of the Asian continent.[16,25,99] In contrast, the oceans adjacent to the Southeast Asian continent show a broadly opposite trend at the precession band regarding rainfall (Figure 5) and rainfall $\delta^{18}O$.[121] This ocean-continent contrast is dubbed the "sea-land precession-phase paradox."[93]

The nonconformity in sea-land precession phases is evident to first order empirically and observationally, but the exact precession phases remain less known. The modeled P_{min}-P_{max} differences theoretically do not provide their precise phases at the precession band. In fact, marine proxy records suggest a large array of potentially different precession phases (~1- to ~10-ka lags to June 21 insolation), which has sparked a longstanding and vigorous dispute, leading to different monsoon hypotheses based on diverse monsoon-insolation

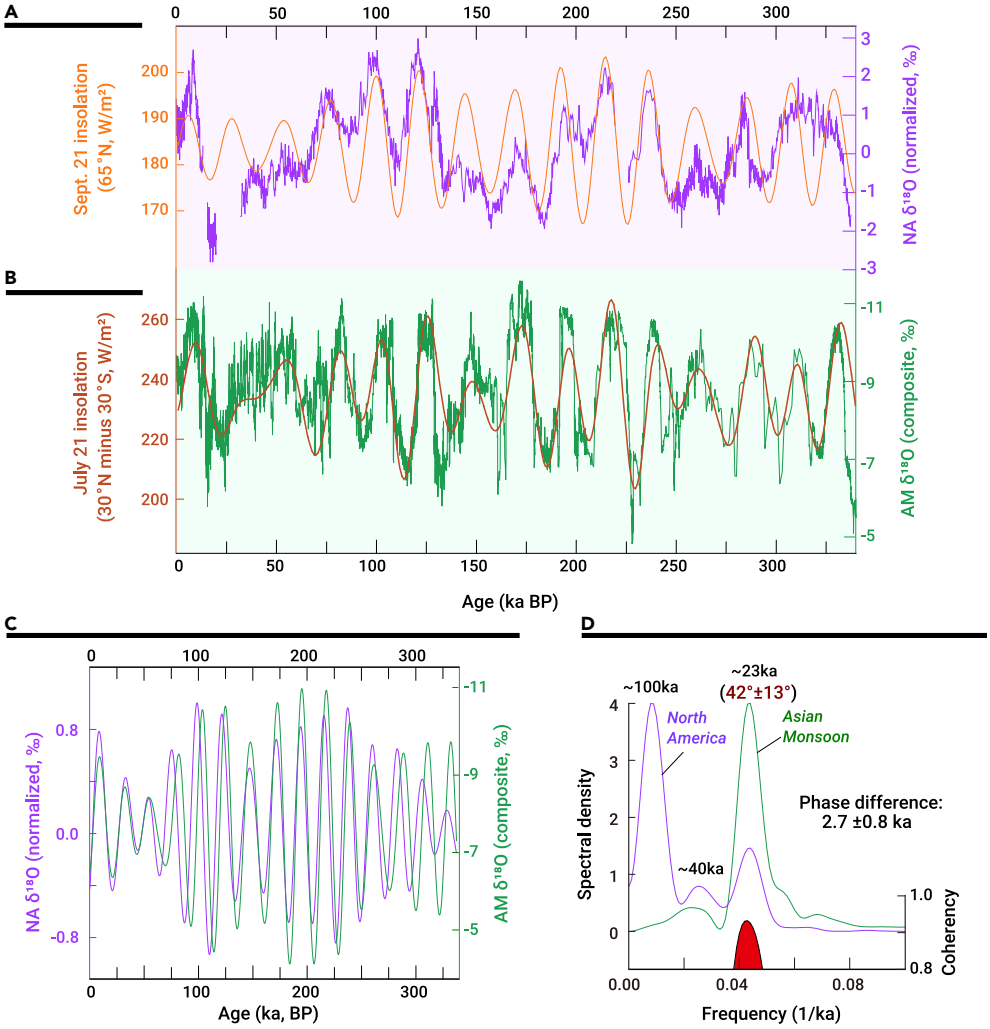

Figure 4. Phase comparison between North American (NA) and AM climate variations at the precession band (A) The normalized NA speleothem $\delta^{18}O$ record (purple)[82] and September 21 insolation at 65° N (orange).[49] (B) The composite AM speleothem $\delta^{18}O$ record (green)[16] and July 21 30° N–30° S insolation (brown).[49] (C) Filtered NA (purple) and AM (green) $\delta^{18}O$ records, using Gaussian filtering at the precession band (frequency, 0.0435; bandwidth, 0.01). (D) Spectral analysis results of NA (purple) and AM (green) $\delta^{18}O$ records and their coherence spectra (red). The AM and NA variations follow ~July 21 and ~September 21 insolation, respectively, with the AM leading NA hydroclimate variations by ~2.7 ± 0.8 ka at the precession band.

relationships.[21,22,40,94,96,112,122–125] These contrasting ideas have hampered full acceptance of the Kutzbach orbital-monsoon hypothesis as an orbital monsoon theory.

The planktonic foraminifera $\delta^{18}O_{sw\text{-}iv\text{-}sst}$ (calibrated $\delta^{18}O$ of sea-surface water based on the reconstructed SST and ice volume isotopic effects) is determined largely by the regional evaporation minus precipitation (E – P).[126] Huang et al.[121] noted that the $\delta^{18}O_{sw\text{-}iv\text{-}sst}$ from the tropical western Pacific shows a broad negative correlation with speleothem $\delta^{18}O$ records from the Asian continent, and they suggested that the strengthened AM at the P_{min} enhanced moisture flux from the western Pacific into the Asian continent and vice versa, contributing to the broad see-saw pattern on the precessional scale. It appears that orbital-scale variations in the $\delta^{18}O_{sw\text{-}iv\text{-}sst}$ over the tropical Pacific and Indian Oceans adjacent to the Asian continent show, to first order, a nearly positive correlation with NHSI (Figure 6), consistent well with model simulations (Figure 5).

As mentioned above, the "sea-land precession-phase paradox" concerns the AM variations on orbital scales with apparent phase differences (~1–10 ka) at the precession band between a wide range of proxy records, including speleothem $\delta^{18}O$ and various marine sediment records in the AM regime (Figures 5 and 6).[15,18,20,25,94,112,122,127–131] A data-model comparison[93] was then used to help the interpretation of the observed phase differences at the precession band among some important continental and marine records, including marine records from the East China Sea (U1429)[21,130] and the Andaman Sea (NGHP17),[112,131] and continental speleothem records[16] that show a significant phase difference at the precession band. More broadly, marine $\delta^{18}O_{sw\text{-}iv\text{-}sst}$ records show, to first order, a nearly positive correlation with NHSI (Figure 5). Therefore, the summer precipitation (evaporation) inferred from these records decreases (increases) over the marine regions when NHSI is high (low) or the overall monsoon is presumably strong (weak). In other words, the rainfall decreases at the precession band over the broad marine regions were compensated by coupled overall rainfall increases over the Asian continent and, thus, actually signify overall strengthening rather than weakening of the AM (Figure 5).[93,121,131,132] This scenario is in line with the strong monsoon circulation under high NHSI inferred by the Asian speleothem $\delta^{18}O$ records.[93] In essence, these seemingly fundamental differences rest in that the sea-land monsoon records characterized different aspects of the same AM system or dynamics.[93]

Recently, another set of marine proxy (e.g., δD, $\delta^{18}O_{sw}$, and Rb/Ca) records from the northwestern Bay of Bengal (U1446) was developed for the past 900 ka.[22,40] These high-quality records suggest a several-thousand-year-long lag of AM (or Indian monsoon [IM]) precipitation or the resultant river runoff and a few-thousand-year-long lag of changes in IM moisture source and transport paths to the summer insolation forcing at the precession band. This core site, as well as the adjacent catchment basins of the Mahanadi and Brahmani rivers that provide the majority of runoffs to the core site, are located at a unique place, according to the model result,[133] where the annual precipitation amount may have different precession phases from the NHSI or the overall precipitation and precipitation $\delta^{18}O$ (commonly correlated with precipitation δD) over the Indian subcontinent (Figure 7).[133] That is, the observed precession phases of the U1446 records[22,40] are consistent with model simulations; although, overall, the Indian subcontinental precipitation amount was higher and precipitation $\delta^{18}O$ (or δD) was lower at 9 ka BP (the high NHSI and strong IM scenario) relative to the preindustrial (PI) state (the low NHSI and weak IM scenario), the behavior across the major Mahanadi-Brahmani catchments and the core site appears to be out of phase. In other words, such a differential among procession phases of the proxy records is plausible, and the model results provided an alternative interpretation in the context of new monsoon dynamics.[93]

Another important progress in monsoon research is a recent model simulation of precession-scale changes in the upwelling along the western Arabian Sea.[134] This involves a classic issue of whether the upwelling intensity (or the related ocean productivity) records from the Arabian Sea[94,96] are a direct expression of IM variability, particularly regarding their precession phases, which considerably lag NHSI.[20] Idealized experiments by fully coupled climate models under different precession configurations show that the area of upwelling is narrow (wide) during high (low) NHSI time or strong (weak) IM times. The underlying mechanism is the effect of convective heating over northeastern Africa and the western equatorial Indian Ocean on the width and meridional location of the low-level jet.[134] Although these sensitivity simulations have difficulty to explore the precession phases precisely, new transient climate simulations on the Arabian Sea upwelling intensity appear to suggest a precession phase approximately opposite to NHSI and, thus, akin to the Arabian Sea records (X. Zhang,

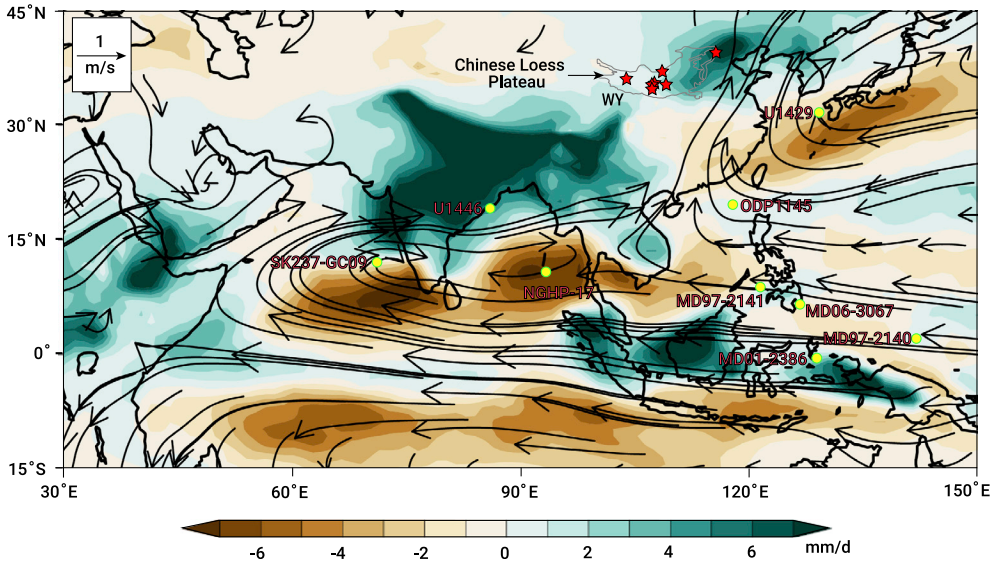

Figure 5. Simulated changes in precipitation rate (mm/day) and 850 hPa wind vectors (m/s) over the AM and adjacent regions during boreal summer (JJA) between the precession minimum (P_{min}) and maximum (P_{max}) from CESM experiments (modified from Shi et al.[12]) The gray line region indicates the Chinese Loess Plateau. Red asterisks indicate locations of major loess-paleosol sections in the Chinese Loess Plateau (including the Jingyuan, Yimaguan, Xifeng, Lingtai, Baoji, Luochuan, and Jingbian sections). The Zhaitang section is at the NE plateau. Yellow dots show marine core locations: MD97-2141,[106] ODP1145,[107] MD06-3067,[108] MD01-2386,[109] U1429,[21] and MD97-2140[110] in the western Pacific and SK237-GC09,[111] U1446,[22] and NGHP17[112] in the Indian Ocean.

personal communication). Therefore, a series of upwelling proxy data obtained over the past ~30 years from the Arabian Sea ultimately has another alternative interpretation in the new interpretative framework in terms of precession phases.[93,134] This new development to some extent explains an important part of the sea-land precession-phase paradox that obstructs acceptance of the Kutzbach orbital monsoon hypothesis.

The "Chinese 100-ka problem"

Another longstanding issue regarding the monsoon hypothesis stems from the Chinese loess magnetic susceptibility (MS) records (as an AM precipitation proxy) from the central Chinese Loess Plateau, which show dominant ~100-ka cycles (or glacial-interglacial cycles),[70] implying a major ice volume forcing of monsoon. This is in contradiction with the conventional insolation hypothesis[8,81] and Chinese speleothem records,[16] namely the "Chinese 100-ka problem."[93] Cheng et al.[93] brought out the non-mainstream notion that MS "flux," rather than the MS, would be a more appropriate proxy of precipitation in principle[135] because it accounts for durations of *in situ* pedogenesis and, thus, matches to the essence of the physical relationship between the magnetic proxy and precipitation. As expected, the MS flux data exhibit more precession power and less 100-ka power compared with the original MS records,[93] which is consistent with a recent spliced loess sand content-MS record.[136] However, the precession power of MS flux data remains less significant than that of the Chinese speleothem records. A closer look at most modeling results shows that the summer rainfall over the Chinese Loess Plateau may be insensitive to precession change,[76,77,115,116,119,120,137] although this could be model dependent because different results have also been found in other models.[69] On the other hand, some model simulations also show that the summer rainfall over the Chinese Loess Plateau is dominated by precession, whereas the annual temperature is more influenced by glacial conditions (CO_2 and ice sheets).[69,70] Therefore, it would be also possible that the loess MS was affected not only by summer precipitation but also by annual temperature and/or other factors/processes.[93,138] A recent study shows that the Tengger desert had also experienced large dry-wet fluctuations with strong 20-ka and 400-ka rhythms as well, probably suggesting East AM (EAM) variations forced dominantly by low-latitude insolation.[139]

The orbital-scale hydroclimate variations in parts of the Indo-Pacific Warm Pool (IPWP), the South China Sea, and the Bay of Bengal appear to show significant ~100-ka glacial-interglacial cycles as inferred by precipitation and precipitation isotope records.[140] Similar to the alternative interpretations for the Bay of Bengal and South China Sea records (Figures 5 and 6),[93] the records from the IPWP (Borneo, Malaysia, and Sumatra, Indonesia) may be tentatively explained by their specific locations in the transition regions between the two "precession regimes" with opposite precipitation amounts and $\delta^{18}O$ variations.[76,77,119] In these regions, like the central Chinese Loess Plateau, muted precession signals may facilitate the powers of other cyclicities. Additionally, the shelf exposure influence because of sea level change on the IPWP hydroclimate is presumably large, affecting regional ocean and atmosphere circulation and amplifying glacial-interglacial cyclicity.[140] The broad anti-phase relationship between NH-SH monsoons on the precession scale implies that the ice volume forcing of monsoons would not be primary because the ice volume forcing is nearly synchronous globally to first order. However, various ice volume forcing effects seem to manifest in the monsoon regime in different ways, particularly in the EAM domain. For example, the ice sheet extent, amplified by the feedback of dust aerosol, can significantly weaken EAM circulation and precipitation.[141] It has also been shown that the effect of ice sheets on the EAM is nonlinear depending on the size and location of the ice sheets and the background insolation.[11,79] Recently, a model simulation[69] has shown that the variation of the summer precipitation over the north of 25° N in the EAM domain is dominated by precession, leading to strong ~23-ka cycles, whereas over the southern part, the ice volume may play an important role in generating ~100-ka cycles by influencing the latitude of the ITCZ and the Hadley cell. These findings from model simulations call for further investigation, especially an in-depth data-model comparison. An thorough understanding of the effect of ice volume/CO_2 forcing on monsoons remains challenging.[69] Sun et al.[70] proposed that "insolation plays a leading role in affecting changes in temperature, precipitation, and southerly wind during the summer season. Changes in annual mean temperature and precipitation are affected to varying degrees by CO_2 and ice volume." Overall, even with addition of ice volume/CO_2 forcing with ~100-ka cycles to the transient simulations, the resultant summer monsoon variations remain predominant with precession cycles in most cases, in line with low-latitude insolation. The main effect of global ice volume/CO_2 forcing seems to lie mainly in the amplitude changes of monsoon variations[12,71,75,93] and/or annual mean temperature and precipitation (or mean state).[70] In principle, the influence of some of the 100-ka variances on the ASM appears to lie mainly in special changes in boundary conditions, such as certain temperature gradients, ITCZ mean position, and land-sea distribution, instead of direct sensitivity to ice volume changes.[142] These explanations eliminate, in part, another critical obstacle, the generalized "Chinese 100-ka problem," to acceptance of the Kutzbach orbital monsoon hypothesis.

Monsoon system science

In the past four decades, researchers have commonly focused on just one specific type of proxy from monsoon regimes, such as the loess MS, marine productivity (upwelling), lake pollen, speleothem $\delta^{18}O$ records, etc. To date, a conventional approach has been to use a specific proxy record or multi-proxy records from an individual location to characterize the entire monsoon system/subsystem exclusively, including monsoon periodicities and dynamics; therefore, such an approach has yielded a wide range of superficial discrepancies in our understanding of monsoon variations on orbital scales, particularly regarding the role of insolation forcing.[20–22,93,127,129,133,142] A large body of valuable data has been amassed, which, together with modeling results, has ultimately led to the end of this era itself. Cheng et al.[93] analogized the monsoon system to a giant "elephant" and suggested that various proxy records from monsoon regimes characterize different but indispensable parts of the same "elephant"— the whole monsoon system. In other words, most of the apparent differences stemmed from interpretations of diverse proxies that are, in essence, not mutually exclusive. In fact, there is an invaluable complementarity between these different proxy records in the interpretative framework of the whole monsoon system in that they

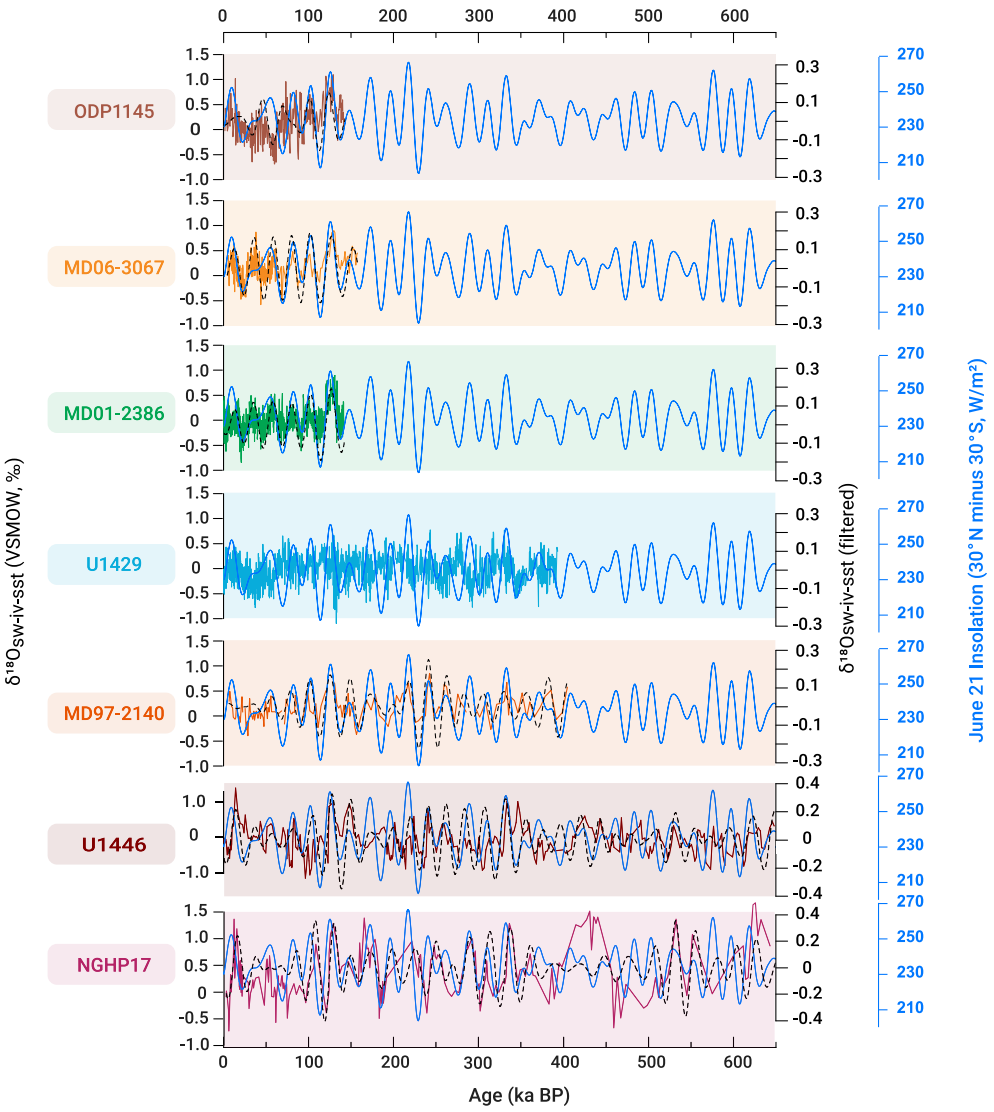

Figure 6. Surface seawater $\delta^{18}O_{sw\text{-}iv\text{-}sst}$ from the Indian Ocean and the western Pacific, and comparison with the June 21 insolation differential between 30° N and 30° S $\delta^{18}O_{sw\text{-}iv\text{-}sst}$ is calculated by removal of SST and global mean ice volume effects from $\delta^{18}O$ of planktonic foraminifera using the mean sea level reconstruction.[48] From top to bottom are ODP1145,[107] MD06-3067,[108] MD01-2386,[109] U1429,[21] and MD97-2140[110] records from the western Pacific region, and U1446[22] and NGHP17[112] records from the Indian Ocean. Dashed lines show data filtered using Gaussian filtering on the precession band (frequency, 0.0435; bandwidth, 0.01). Blue curves show the differential between 21 June insolation at 30° N and 30° S. $\delta^{18}O_{sw\text{-}iv\text{-}sst}$ variations respond primarily to local E-P as well as river runoff in some cases. It appears that the $\delta^{18}O_{sw\text{-}iv\text{-}sst}$ records show an overall positive correlation with the June insolation, suggesting a general E-P increase with the increase in summer insolation over the broad oceanic regions in the AM domain. The U1429 record shows almost no precessional variance,[21] which is consistent with model results that suggest a weak precessional variance in rainfall and runoff originating from the Yangtze River Valley (Figure 5).[93]

describe distinct dynamic aspects of the same monsoon system and, therefore, are linked closely to each other despite the superficial differences; for instance, in periodicities and precession phases as discussed above. Collectively, the discrete dynamic nature of monsoon calls for a new systematic approach in monsoon research or "monsoon system science" to better understand how the different pieces of the monsoon system work and interact in the context of data syntheses on the monsoon regime scale. Analogous to the legend of "blind men and giant elephant," a whole, not a partial, view of the monsoon system becomes critical. Therefore, although each climate record is always important, a simple generalization/exemplification from a single record to the whole monsoon system is evidently an outdated approach. This development propels a change in monsoon research to a systematic paradigm or monsoon system science, which underlines a systematic/integrative view of different dynamic natures/responses/feedback across an exceptionally broad range of temporospatial scales in a monsoon system and put them into the context of external insolation and internal (ice volume/CO_2) forcings. This development, including explanations of the two paradoxes mentioned above, may be a decisive step toward acceptance of the Kutzbach orbital monsoon hypothesis as a theory addressing the key aspect of monsoon climates.

ICE SHEET AND MONSOON INTERPLAY

The Milankovitch theory postulates that changes in the high-latitude NHSI drive variances in Late Quaternary ice sheet extent, which, in turn, incite ancillary changes in other parts of the global climate system. In the Earth's tropics-subtropics, however, the monsoon variations are largely driven by tropical-subtropical insolation and manifest as inter-hemispherical anti-phased precession cycles. This dual nature in orbital forcings and their hydroclimate responses/feedback are distinctive, but their interplay is inevitable and complex as well. In the following discussions, we enumerate several relevant issues.

The pattern of glacial-interglacial temperature variations

The most prominent feature of global climate change is the broad similarity between global temperature and atmospheric CO_2 variations

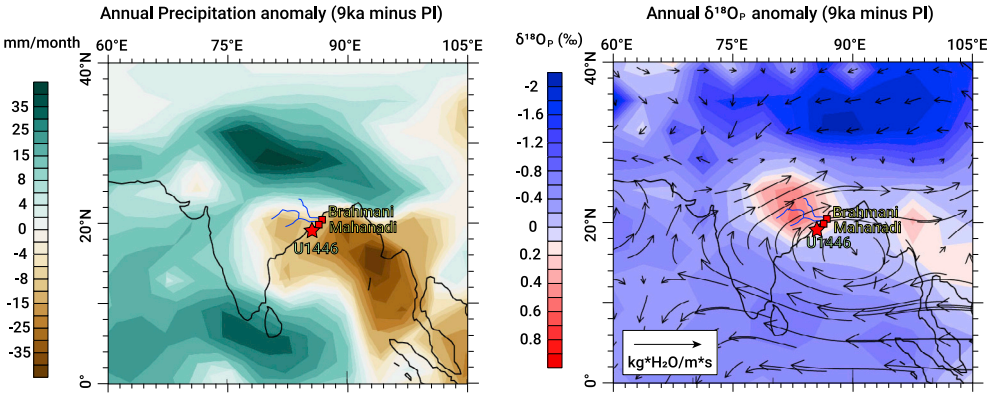

Figure 7. Simulated differences of annual precipitation, annual precipitation $\delta^{18}O$, and 850-hPa water vapor transport between 9 ka and PI from the COSMOS-wiso The red star depicts the IODP U1446 location. The major parts of the Mahanadi and Brahmani rivers (blue lines) and their coastal outlets (red squares) are shown. Although the overall continental precipitation amount was higher and precipitation $\delta^{18}O$ was lower at 9 ka (high NHSI and strong AM) relative to the PI (low NHSI and weak AM), the behavior across the major Mahanadi and Brahmani catchments and the IODP U1446 site are considerably out of phase. These modeling results agree broadly with the observations from the U1446 records.[22,40] Modified from Zhang et al.[133]

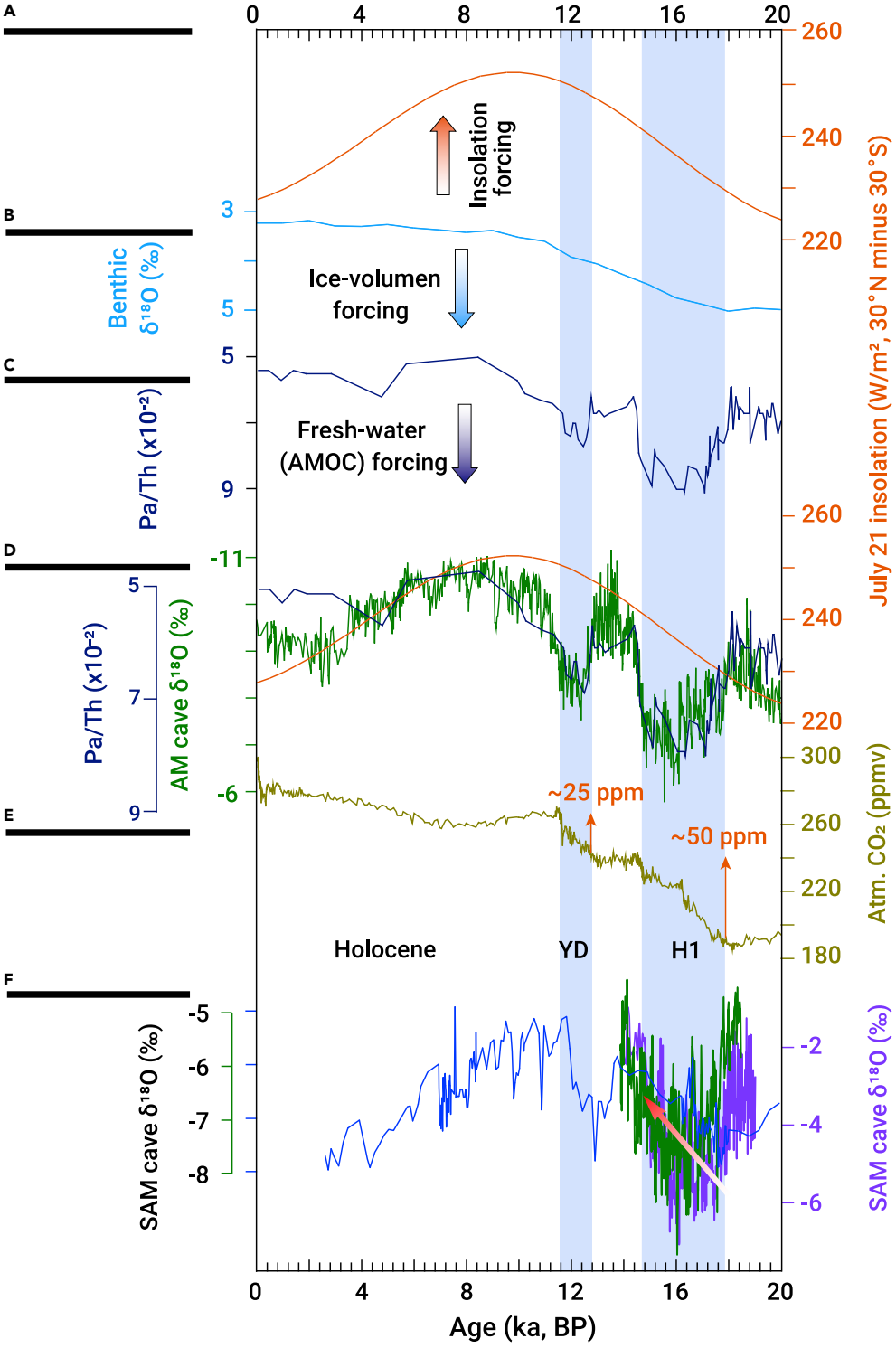

Figure 8. The AM forcings across the last deglaciation process (A) The insolation forcing is depicted by 30° N–30° S July 21 insolation.[49] (B) Ice volume forcing is inferred from the stacked benthic $\delta^{18}O$ record.[7] (C) Freshwater (or AMOC) forcing is inferred by $^{231}Pa/^{230}Th$ ratios of marine sediments.[152,153] (D) Comparison of insolation (orange)[49] and AMOC (dark blue)[152,153] forcings and their effects on the AM variations (green).[16] (E) Atmosphere CO_2 concentration.[151,154] Orange arrows show CO_2 increases across the YD and HS1. (F) SAM cave $\delta^{18}O$ records (blue,[80] green and purple[155]) show a persistent dry trend across HS1 (red arrow).

on the glacial-interglacial scale globally. For example, the long-term variations of Antarctic temperature are virtually as same as the global ice volume/CO_2 or northern high-latitude temperature changes.[7,143] The SST records across the NH-SH also show patterns broadly similar[144] to the ice volume and Antarctic temperature, consistent with the *sensu lato* Milankovitch theory: the ice sheet effect on global climate (particularly the changes in the temperature pattern). The observation that changes in the northern high-latitude ice sheet drive global temperature variations predominantly in a similar pattern on the glacial-interglacial scale is important for a better understanding of monsoon dynamics. This is because changes in the temperature gradient (and, in turn, atmosphere-ocean circulation) are likely more important to monsoon dynamics to first order than similar temperature changes associated with glacial-interglacial cycles.[12]

The AM and Antarctic temperature variations are broadly similar on the millennial scale, with a broad anti-phased variability (Figure 1C). As suggested previously, the AM is influenced by a combination of NH "pull" and SH "push" mechanisms.[16,100–102,145] The essence of these mechanisms rests on the influence of the interhemispheric temperature gradient on the monsoon variability on the millennial scale, which is comparable mechanistically with the similar driving forcing of monsoon on the orbital scale: the interhemispheric insolation differential (e.g., the SITIG[97] or 30° N–30° S[98,99]).

CH_4 and CO_2 feedback

It has long been recognized that atmospheric CO_2 change, although mechanistically complex,[146] has a very close relationship with global sea level/ice volume changes, and at the precession band, it is approximately in phase with the NH September insolation (~5-ka lag to NH June 21 insolation) (Figure 4).[143,146,147] On the other hand, the AM speleothem $\delta^{18}O$[16] and ice core CH_4 records[148] show prominent precession pacing of low-latitude hydroclimate changes with a nearly in-phase relation with the NH July insolation (~2- to 3-ka lag to NH June 21 insolation) at the precession band. This phase relation between AM and CH_4 supports the notion that greenhouse gas CH_4 responses to the NH monsoon change without observable lags,[16,79,149,150] suggesting early CH_4 feedback at the precession band compared with the ice volume and CO_2 in the Earth's climate system or a potential low- to high-latitude directionality of climate interaction.

On the other hand, the rapid CO_2 increase[151] as a critical feedback during the last deglaciation could be also critical for the full glacial termination; for example, it might have propelled the deglaciation striding across the cooling periods of the Younger Dryas (YD) (with an ~25 ppm CO_2 increase) and Heinrich stadial 1 (HS1) (with an ~50 ppm CO_2 increase) (Figure 8E).[151,154] This is because, mechanistically, an ~15 ppm CO_2 rise during a millennial-scale event (e.g., YD and HS1) is sufficient to alter atmospheric moisture transport across Central America and, subsequently, modulate the North Atlantic freshwater budget, ultimately resulting in transition from a weak to a strong AMOC mode and, in turn, intensified AM (Figure 8).[156] Essentially, these processes indicate a high- to low-latitude directionality of climate interaction.

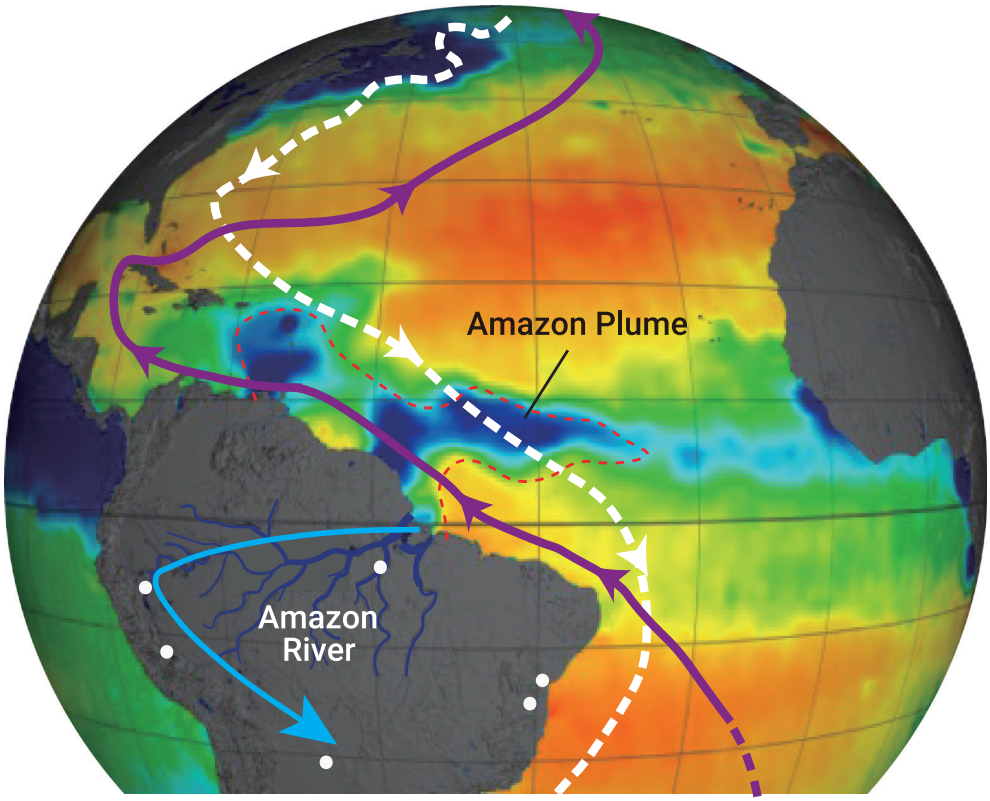

Figure 9. Conceptual diagram depicting the climatic dynamics during termination of the millennial-scale climate events. Based on cave records,[150,161] the weakened SAM resulted in reduced Amazon River runoff into the tropical Atlantic Ocean and, thus, a small Amazon plume region (APR; depicted by the red dashed line) about multi-centuries prior to the millennial event termination at Greenland. The long-term drying trend in the SAM domain may have induced a relatively positive SSS anomaly in the APR, which was subsequently advected to the North Atlantic,[162,163] ultimately contributing to AMOC strengthening.[164,165] White dots show locations of cave records. Purple and white arrows indicate the surface and deep ocean currents, respectively. The light blue arrow depicts the wind direction of the SAM. This figure is modified from Cheng et al.[150] and Dong et al.[161] The map shows surface salinity in 2011 as measured by the National Aeronautics and Space Administration (NASA) Aquarius satellite. Orange colors indicate higher salinity and blue colors lower salinity (https://news.uga.edu/wp-content/uploads/2017/12/Amazon-River-Plume.jpg).

The phase relation between the AM and the ice sheet at the precession band

As mentioned previously, a close comparison of precession phases between absolutely dated AM[16] and North American hydroclimate[82] records revealed that the AM led the North American hydroclimate (or ice sheet) by ~2.7 ± 0.8 ka at the precession band (Figure 4). This observation suggests a more active role of low-latitude monsoons in driving global hydroclimate change than previously thought.[13–15,67,73,97,99] That is, at the precession band, low-latitude monsoons appear to be an important driver of global hydroclimate changes, including their potential influence on the high-latitude hydroclimate via input of water vapor and CH_4 to the atmosphere and transport of heat to high latitude through ocean circulation (such as the AMOC).[25,62,72,73,99]

The role of the AMOC

During the past two decades, the high- and low-latitude climate teleconnections at multiple timescales have been well established empirically and theoretically. One convincing piece of evidence comes from the precise correlation between the millennial-scale events recorded in Greenland ice core and AM speleothem records.[16,50,149,150] The key process underlying this teleconnection lies in the AMOC dynamics (less in direct ice volume forcing), which links changes in high-latitude temperature to low-latitude monsoon intensity. For example, as inferred by $^{231}Pa/^{230}Th$ records[152,157,158] over the last deglaciation process, the high-latitude weak AMOC events associated with HS1 and YD affected the AM profoundly, resulting in pronounced weak monsoon intervals, whereas the influence of a persistent decrease of the ice volume was tentative (Figure 8). In particular, while the ice volume around 18–19 ka BP was very close to its maximum, the AM reached an apparent peak, coherent with the strong AMOC peak, which is clearly not in tune with the ice volume variance (Figure 8). In other words, the ice volume effect appears to be less effective in terms of driving monsoon changes. Nevertheless, provided that the ice volume changes affect the AMOC (very likely) via changing the North Atlantic meltwater forcing for instance, therewith the monsoon will respond much more sensitively. In this respect, the ice volume change rate and the trajectory/distribution of the resultant meltwater in the North Atlantic, not the ice volume per se, would be more critical for low-latitude monsoons.[159] In a pioneer modeling study, Kutzbach and Guetter[78] showed that "the response of monsoon circulations and tropical precipitation to the orbitally produced solar radiation changes was much larger than the response to changes of glacial-age boundary conditions." In their experiment, the glacial-age boundary conditions include the ice sheet and related land albedo, sea ice, and SST conditions but not AMOC, consistent with the observations. Another example is a recent model simulation that also suggests that the abrupt low-latitude monsoon weakening events that occurred during the ending processes of interglacials were associated with the astronomically triggered abrupt weakening of the AMOC[160] rather than with a direct ice volume change.

SAM (Amazon River discharge)

Recent studies show that, during the termination processes of millennial-scale events such as HSs, a multi-centennial drying trend occurred as a precursor event in the vast SAM domain, which would have caused a decrease in Amazon River discharge into the tropical Atlantic Ocean (Figures 8 and 9).[150,161] Reduced freshwater input may have induced a positive sea-surface salinity anomaly in the huge Amazon plume region,[166,167] ultimately advected to the deep-water formation areas in the North Atlantic via the great ocean conveyor[162] and contributing to the strengthening of the AMOC[164,165] and vice versa. A strengthened AMOC would induce positive feedback by transporting more saline water to the north, facilitating northward heat transport and a shift in the tropic rain belts, intensification of the AM,[62,149,150,161] and Greenland warming.[168] This dynamic process provides another example showing that low-latitude monsoon rainfall may affect high-latitude climate.

PROSPECT

The Milankovitch theory became an accepted version of the astronomical theory of climate change mainly because the major periodicities of the astronomical parameters were found to be consistent with the geological records of the northern high-latitude ice sheets, and, subsequently, the ice sheets forced nearly coincident global climate changes. However, orbital-scale climate changes of Earth are not dictated by high-latitude ice sheets alone. In fact, more than half a century before Milankovitch's seminal study,[1] Adhémar[169] and Croll[170] had hypothesized hemispherically asymmetric occurrences of ice ages at precession periods. Although their hypotheses were eventually discarded because of observations that are consistent with the hemispherical coincidence of ice ages and summer, rather than winter, insolation is the most favorable. The core concept that precession-driven changes in insolation drive asynchronous (or anti-phased) hydroclimate fluctuations in the NH and SH found support in the 1980s, when Kutzbach[8] put forth a simple hypothesis that summer insolation drives monsoon variance: the Kutzbach orbital monsoon hypothesis.[13] This hypothesis is now tested by empirical and observational data, especially the decisive and elegant evidence from low-latitude

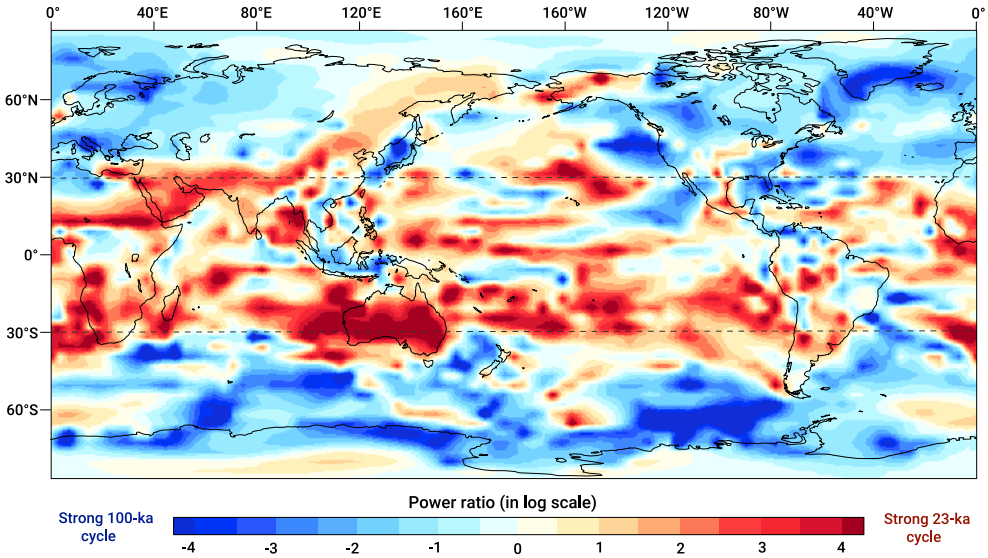

Figure 10. Simulated 23- and 100-ka cycle power ratios of annual precipitation illustrate the dual nature of global hydrodynamics in the high- and low-latitude regimes on orbital scales Shown is simulated cyclicality of annual precipitation variations for the past 300 ka. The transient simulations were initialized from the PI conditions and forced by the orbital (ORB) and greenhouse gas (GHG) forcings as well as the prescribed fluctuations of continental ice sheets (ICE) for the past 300 ka.[171] The simulated precipitation time series over each model grid cell was calculated to attain the power spectrum of annual precipitation for each grid cell, and the results were used to estimate the distribution of ~23-ka and ~100-ka band-average power. The natural log of this ratio is presented here so that the positive/negative values indicate that the 23-ka cycle of annual precipitation variabilities was stronger/weaker than the 100-ka cycle. The global annual precipitations show stronger ~23-ka cycles in low-latitude regions (~30° N–30° S, depicted by dashed lines), in contrast to high-latitude regions, where ~100-ka cycles are stronger.

monsoon variability inferred, for example, from Asian[16,51] and South American[74,80] speleothem records. We therefore call for a combined Milankovitch-Kutzbach hypothesis— a unified framework for understanding orbital-scale global climate variability. This form of orbital hypothesis not only accentuates that high-latitude NH summer insolation drives changes in ice sheet extent at the Earth's orbital periods and its nearly synchronous effect globally on glacial-interglacial variability but also emphasizes that inter-tropical insolation differential drives inter-hemispherically out-of-phase low-latitude hydroclimate variability at the precession band (Figure 10). Basically, we suggest blending the global monsoon with the existing framework of the orbital theory to formulate a more comprehensive interpretative framework of Earth's orbital climate changes, including the dual nature of orbital hydrodynamics of the high-latitude ice sheet and low-latitude monsoon in the context of the dual insolation forcings and their broad interplays (Figure 10). To advance the Milankovitch-Kutzbach hypothesis into a new accepted version of the astronomical theory of climate, there is much more to be done, such as gaining a better understanding of the global-scale low- and high-latitude interactions and feedback and, in particular, research on the forefront of "monsoon system science"— a new monsoon research paradigm.

REFERENCES

1. Milankovitch, M.K. (1941). Canon of Insolation and the Ice Age Problem (Royal Serbian Academy Special Publication). (in German).
2. Hays, J.D., Imbrie, J., and Shackleton, N.J. (1976). Variations in the earth's orbit: pacemaker of the ice ages. Science ***194***, 1121–1132.
3. Berger, A.L. (1977). Support for the astronomical theory of climatic change. Nature ***269***, 44–45.
4. Imbrie, J., Hayes, J.D., Martrinson, D.G., et al. (1984). The orbital theory of Pleistocene climate: support from a revised chronology of the marine $\delta^{18}O$ record. In Milankovitch and Climate Part I (D. Reidel Publishing Company), pp. 269–305.
5. Imbrie, J., McIntyre, A., and Mix, A. (1989). Oceanic response to orbital forcing in the late Quaternary: observational and experimental strategies. In Climate and Geo-Sciences (Springer), pp. 121–164.
6. Imbrie, J., Boyle, E.A., Clemens, S.C., et al. (1992). On the structure and origin of major glaciation cycles 1. Linear responses to Milankovitch forcing. Paleoceanography ***7***, 701–738.
7. Lisiecki, L.E., and Raymo, M.E. (2005). A Pliocene-Pleistocene stack of 57 globally distributed benthic $\delta^{18}O$ records. Paleoceanography ***20***, PA1003. https://doi.org/10.1029/2004PA001071.
8. Kutzbach, J.E. (1981). Monsoon climate of the early Holocene: climate experiment with the earth's orbital parameters for 9000 years ago. Science ***214***, 59–61.
9. Kutzbach, J.E., and Street-Perrott, F.A. (1985). Milankovitch forcing of fluctuations in the level of tropical lakes from 18 to 0 kyr BP. Nature ***317***, 130–134.
10. Prell, W.L., and Kutzbach, J.E. (1987). Monsoon variability over the past 150, 000 years. J. Geophys. Res. ***92***, 8411–8425.
11. Berger, A., Driesschaert, E., Goosse, H., et al. (2008). The Eurasian ice sheet reinforces the East Asian summer monsoon during the interglacial 500, 000 years ago. Clim. Past ***4***, 79–90.
12. Shi, Z.G., Lei, Q., and Zhou, P. (2020). Numerical simulation researches on orbital-scale Asian climate dynamics; history and perspective (in Chinese). Quat. Sci. ***40***, 8–17.
13. Ruddiman, W.F. (2006a). Orbital changes and climate. Quat. Sci. Rev. ***25***, 3092–3112.
14. Kutzbach, J.E., Liu, X., Liu, Z., and Chen, G. (2008). Simulation of the evolutionary response of global summer monsoons to orbital forcing over the past 280, 000 years. Clim. Dyn. ***30***, 567–579. https://doi.org/10.1007/s00382-007-0308-z.
15. Cheng, H., Sinha, A., Wang, X.F., et al. (2012a). The global paleomonsoon as seen through speleothem records from asia and south America. Clim. Dyn. ***39***, 1045–1062.
16. Cheng, H., Edwards, R.L., Sinha, A., et al. (2016a). The Asian monsoon over the past 640, 000 years and ice age terminations. Nature ***534***, 640–646.
17. Wang, P.X., Wang, B., Cheng, H., et al. (2014). The global monsoon across timescales: coherent variability of regional monsoons. Clim. Past ***10***, 2007–2052.
18. Wang, P.X., Wang, B., Cheng, H., et al. (2017). The global monsoon across time scales: mechanisms and outstanding issues. Earth Sci. Rev. ***174***, 84–121.
19. Broecker, W.S., and VanDonk, J. (1970). Insolation changes, ice volumes and the O^{18} in deep-sea cores. Rev. Geophys. ***8***, 169–198.
20. Ruddiman, W.F. (2006b). What is the timing of orbital-scale monsoon changes? Quat. Sci. Rev. ***25***, 657–658.
21. Clemens, S.C., Holbourn, A., Kubota, Y., et al. (2018). Precession-band variance missing from East Asian monsoon runoff. Nat. Commun. ***9***, 3364.
22. Clemens, S.C., Yamamoto, M., Thirumalai, K., et al. (2021). Remote and local drivers of Pleistocene South Asian summer monsoon precipitation: a test for future predictions. Sci. Adv. ***7***, eabg3848.
23. Cheng, H., Lawrence Edwards, R., Shen, C.C., et al. (2013a). Improvements in ^{230}Th dating, ^{230}Th and ^{234}U half-life values, and U-Th isotopic measurements by multi-collector inductively coupled plasma mass spectrometry. Earth Planet Sci. Lett. ***371–372***, 82–91.
24. Henderson, G.M. (2006). Climate-Caving in to new chronologies. Science ***313***, 620–622.
25. Cheng, H.W., Zhang, H., Zhao, J.Y., et al. (2019a). Chinese stalagmite paleoclimate researches: a review and perspective. Sci. China Earth Sci. ***62***, 1489–1513.
26. Elkibbi, M., and Rial, J.A. (2001). An outsider's review of the astronomical theory of the climate: is the eccentricity-driven insolation the main driver of the ice ages? Earth Sci. Rev. ***56***, 161–177.
27. Berger, A., and Loutre, M.F. (1991). Insolation values for the climate of the last 10 million years. Quat. Sci. Rev. ***10***, 297–317.
28. Lisiecki, L.E. (2010). Links between eccentricity forcing and the 100, 000-year glacial cycle. Nat. Geosci. ***3***, 349–352.
29. Huybers, P., and Wunsch, C. (2005). Obliquity pacing of the late Pleistocene glacial terminations. Nature ***434***, 491–494.
30. Bintanja, R., and van de Wal, R.S.W. (2008). North American ice-sheet dynamics and the onset of 100, 000-year glacial cycles. Nature ***454***, 869–872.
31. Bajo, P., Drysdale, R.N., Woodhead, J.D., et al. (2020). Persistent influence of obliquity on ice age terminations since the Middle Pleistocene transition. Science ***367***, 1235–1239.
32. Imbrie, J., and Imbrie, J.Z. (1980). Modeling the climatic response to orbital variations. Science ***207***, 943–953.
33. Paillard, D. (1998). The timing of Pleistocene glaciations from a simple multiple-state climate model. Nature ***391***, 378–381.
34. Huybers, P. (2011). Combined obliquity and precession pacing of late Pleistocene deglaciations. Nature ***480***, 229–232.
35. Raymo, M.E. (1998). Glacial puzzles. Science ***281***, 1467–1468.
36. Maslin, M.A., and Ridgewell, A.J. (2005). Mid-Pleistocene revolution and the 'eccentricity myth'. In Early-Middle Pleistocene Transitions: The Land-Ocean Evidence, M.J. Head and P.L. Gibbard, eds. (Geological Society of London), pp. 19–34.
37. Saltzman, B., Hansen, A.R., and Maasch, K.A. (1984). The late Quaternary glaciations as the response of a three-component feedback system to Earth-orbital forcing. J. Atmos. Sci. ***41***, 3380–3389.

38. Toggweiler, J.R. (2008). Origin of the 100, 000-year timescale in Antarctic temperatures and atmospheric CO_2. Paleoceanography ***23***, PA2211.
39. Nie, J.S., King, J., and Fang, X.M. (2008). Late pliocene–early Pleistocene 100-ka problem. Geophys. Res. Lett. ***35***, L21606.
40. McGrath, S.M., Clemens, S.C., Huang, Y., and Yamamoto, M. (2021). Greenhouse gas and ice volume drive Pleistocene Indian Summer Monsoon precipitation isotope variability. Geophys. Res. Lett. ***48***, e2020GL092249.
41. Bouttes, N., Paillard, D., Roche, D.M., et al. (2012). Impact of oceanic processes on the carbon cycle during the last termination. Clim. Past ***8***, 149–170.
42. Paillard, D., and Parrenin, F. (2004). The Antarctic ice-sheet and the triggering of deglaciations. Earth Planet Sci. Lett. ***227***, 263–271.
43. Tzedakis, P.C., Crucifix, M., Mitsui, T., and Wolff, E.W. (2017). A simple rule to determine which insolation cycles lead to interglacials. Nature ***542***, 427–432.
44. Berger, A., and Loutre, M.F. (1994). In Precession, Eccentricity, Obliquity, Insolation and Paleoclimates. NATO ASI Series, *I 22*, J.C. Duplessy and M.T. Spyridakis, eds. (Springer-Verlag Berlin Heidelberg), pp. 107–151.
45. Berger, A., Li, X., and Loutre, M.F. (1999). Modelling northern hemisphere ice volume over the last 3 Ma. Quat. Sci. Rev. ***18***, 1–11.
46. Roe, G. (2006). In defense of Milankovitch. Geophys. Res. Lett. ***33***, L24703.
47. Berger, W.H. (2012). Milankovitch Theory—Hits and Misses (Scripps Institution of Oceanography Technical Report).
48. Spratt, R.M., and Lisiecki, L.E. (2016). A late Pleistocene sea level stack. Clim. Past ***12***, 1079–1092.
49. Laskar, J., Robutel, P., Joutel, F., et al. (2004). A long-term numerical solution for the insolation quantities of the Earth. Astron. Astrophys. ***428***, 261–285.
50. Cheng, H., Edwards, R.L., Wang, Y., et al. (2006). A penultimate glacial monsoon record from Hulu Cave and two-phase glacial terminations. Geol. ***34***, 217–220.
51. Cheng, H., Edwards, R.L., Broecker, W.S., et al. (2009). Ice age terminations. Science ***326***, 248–252.
52. Berger, A. (1978). Long-term variations of daily insolation and Quaternary climatic changes. J. Atmos. Sci. ***35***, 2362–2367.
53. Wolff, E.W., Fischer, H., and Röthlisberger, R. (2009). Glacial terminations as southern warmings without northern control. Nat. Geosci. ***2***, 206–209.
54. Barker, S., Knorr, G., Edwards, R.L., et al. (2011). 800, 000 years of abrupt climate variability. Science ***334***, 347–351.
55. Schaefer, J.M., Putnam, A.E., Denton, G.H., et al. (2015). The southern glacial maximum 65, 000 years ago and its unfinished termination. Quat. Sci. Rev. ***114***, 52–60.
56. Imbrie, J., Berger, A., Boyle, E.A., et al. (1993). On the structure and origin of major glaciation cycles: 2. The 100, 000-year cycle. Paleoceanography ***8***, 699–735.
57. Raymo, M.E. (1997). Timing of major climate terminations. Paleoceanography ***12***, 577–585.
58. Parrenin, F., and Paillard, D. (2003). Amplitude and phase of glacial cycles from a conceptual model. Earth Planet Sci. Lett. ***214***, 243–250.
59. Abe-Ouchi, A., Saito, F., Kawamura, K., et al. (2013). Insolation-driven 100, 000-year glacial cycles and hysteresis of ice-sheet volume. Nature ***500***, 190–193.
60. Barker, S., Starr, A., van der Lubbe, J., et al.; IODP Exp 361 Shipboard Scientific Party† (2022). Persistent influence of precession on northern ice sheet variability since the early Pleistocene. Science ***376***, 961–967.
61. Stocker, T.F., and Johnsen, S.J. (2003). A minimum model for the bipolar seesaw. Paleoceanography ***18***, PA1087.
62. Zhang, X., Barker, S., Knorr, G., et al. (2021). Direct astronomical influence on abrupt climate variability. Nat. Geosci. ***14***, 819–826.
63. Adler, R.F., Sapiano, M., Huffman, G.J., et al. (2018). The Global Precipitation Climatology Project (GPCP) monthly analysis (new version 2.3) and a review of global precipitation. Atmosphere ***9***, 138.
64. Wang, B., and Ding, Q. (2008). Global monsoon: dominant mode of annual variation in the tropics. Dyn. Atmos. Oceans ***39***, 165–168.
65. Yoshimura, K., Kanamitsu, M., Noone, D., and Oki, T. (2008). Historical isotope simulation using reanalysis atmospheric data. J. Geophys. Res. ***113***, D19108.
66. Trenberth, K.E., Stepaniak, D.P., and Caron, J.M. (2000). The global monsoon as seen through the divergent atmospheric circulation. J. Clim. ***13***, 3969–3993.
67. Wang, P.X. (2009). Global monsoon in a geological perspective. Sci. Bull. ***54***, 1113–1136.
68. An, Z.S., Wu, G.X., Li, J.P., et al. (2015). Global monsoon dynamics and climate change. Annu. Rev. Earth Planet Sci. ***43***, 29–77.
69. Lyu, A.Q., Yin, Q.Z., Crucifix, M., and Sun, Y.B. (2021). Diverse regional sensitivity of summer precipitation in East Asia to ice volume, CO_2 and astronomical forcing. Geophys. Res. Lett. ***48***, e2020GL092005.
70. Sun, Y.B., Wang, T., Yin, Q.Z., et al. (2022). A review of orbital-scale monsoon variability and dynamics in East Asia during the Quaternary. Quat. Sci. Rev. ***288***, 107593.
71. Huang, E.Q., Wang, P.X., Wang, Y., et al. (2020). Dole Effect as a measurement of the low-latitude hydrological cycle over the past 800 thousand years. Sci. Adv. ***6***, eaba4823.
72. Wang, P.X. (2006). Orbital forcing of the low-latitude processes (in Chinese). Quat. Sci. ***26***, 694–708.
73. Wang, P.X. (2021). Low-latitude forcing: a new insight into paleo-climate changes. Innovation ***2***, 100145.
74. Cruz, F.W., Burns, S.J., Karmann, I., et al. (2005). Insolation-driven changes in atmospheric circulation over the past 116, 000 years in subtropical Brazil. Nature ***434***, 63–66.
75. Weber, S.L., and Tuenter, E. (2011). The impact of varying ice sheets and greenhouse gases on the intensity and timing of boreal summer monsoons. Quat. Sci. Rev. ***30***, 469–479.
76. Bosmans, J.H.C., Erb, M.P., Dolan, A.M., et al. (2018). Response of the Asian summer monsoons to idealized precession and obliquity forcing in a set of GCMs. Quat. Sci. Rev. ***188***, 121–135.
77. Hu, J., Emile-Geay, J., Tabor, C., et al. (2019). Deciphering oxygen isotope records from Chinese speleothems with an isotope-enabled climate model. Paleoceanogr. Paleoclimatol. ***34***, 2098–2112.
78. Kutzbach, J.E., and Guetter, P.J. (1986). The influence of changing orbital parameters and surface boundary conditions on climate simulations for the past 18, 000 years. J. Atmos. Sci. ***43***, 1726–1759.
79. Yin, Q.Z., Berger, A., and Crucifix, M. (2009). Individual and combined effects of ice sheets and precession on MIS-13 climate. Clim. Past ***5***, 229–243.
80. Cheng, H., Sinha, A., Cruz, F.W., et al. (2013b). Climate change patterns in South America over the past 250 ka and tropical biodiversity. Nat. Commun. ***4***, 1411.
81. Ruddiman, W.F. (2003). Orbital insolation, ice volume, and greenhouse gases. Quat. Sci. Rev. ***22***, 1597–1629.
82. Cheng, H., Springer, G.S., Sinha, A., et al. (2019b). Eastern North American climate in phase with fall insolation throughout the last three glacial-interglacial cycles. Earth Planet Sci. Lett. ***522***, 125–134.
83. Bhattacharya, T., Tierney, J.E., and DiNezio, P. (2017). Glacial reduction of the North American Monsoon via surface cooling and atmospheric ventilation. Geophys. Res. Lett. ***44***, 5113–5122.
84. Bar-Matthews, M., Ayalon, A., Gilmour, M., et al. (2003). Sea–land oxygen isotopic relationships from planktonic foraminifera and speleothems in the Eastern Mediterranean region and their implication for paleorainfall during interglacial intervals. Geochim. Cosmochim. Acta ***67***, 3181–3199.
85. Mehterian, S., Pourmand, A., Sharifi, A., et al. (2017). Speleothem records of glacial/interglacial climate from Iran forewarn of future Water Availability in the interior of the Middle East. Quat. Sci. Rev. ***164***, 187–198.
86. Wang, H.B., Wang, X.Y., Pérez-Mejías, C., et al. (2022). Orbital-scale hydroclimate variations in the southern Tibetan Plateau over the past 414, 000 years. Quat. Sci. Rev. ***291***, 107658.
87. Shi, Z.G., Zhou, P., Li, X.Z., et al. (2021). Distinct Holocene precipitation trends over arid Central Asia and linkages to westerlies and Asian monsoon. Quat. Sci. Rev. ***266***, 107055.
88. Cheng, H., Zhang, P.Z., Spötl, C., et al. (2012b). The climate cyclicity in arid central Asia over the past 500, 000 years. Geophys. Res. Lett. ***39***, L01705.
89. Cheng, H., Spötl, C., Breitenbach, S.F.M., et al. (2016b). Climate variations of Central Asia on orbital to millennial timescales. Sci. Rep. ***5***, 36975.
90. Cheng, H., Li, H.Y., Zhang, X., et al. (2020a). European-Asian-African continent: an early form of supercontinent and supermonsoon. Quat. Sci. ***40***, 1381–1396.
91. Shi, Z.G., Liu, X.D., Sun, Y.B., et al. (2011). Distinct responses of East Asian summer and winter monsoons to astronomical forcing. Clim. Past ***7***, 1363–1370.
92. Ziegler, M., Tuenter, E., and Lourens, L.J. (2010). The precession phase of the boreal summer monsoon as viewed from the eastern Mediterranean (ODP Site 968). Quat. Sci. Rev. ***29***, 1481–1490.
93. Cheng, H., Zhang, H.W., Cai, Y.J., et al. (2021a). Orbital-scale Asian summer monsoon variations: paradox and exploration. Sci. China Earth Sci. ***64***, 529–544. https://doi.org/10.1007/s11430-020-9720-y.
94. Clemens, S., Prell, W., Murray, D., et al. (1991). Forcing mechanisms of the Indian Ocean monsoon. Nature ***353***, 720–725.
95. Clemens, S.C., Murray, D.W., and Prell, W.L. (1996). Nonstationary phase of the plio-pleistocene asian monsoon. Science ***274***, 943–948.
96. Clemens, S.C., and Prell, W.L. (2003). A 350000 year summer-monsoon multi-proxy stack from the owen ridge, northern Arabian Sea. Mar. Geol. ***201***, 35–51.
97. Reichart, G.J. (1997). Late Quaternary variability of the Arabian Sea monsoon and oxygen minimum zone (in German). Geoloica Ultraiectina ***154***, 1–174.
98. Zhou, W., Priller, A., Beck, J.W., et al. (2007). Disentangling geomagnetic and precipitation signals in an 80-kyr Chinese loess record of ^{10}Be. Radiocarbon ***49***, 137–158.
99. Beck, J.W., Zhou, W., Li, C., et al. (2018). A 550, 000-year record of East Asian monsoon rainfall from ^{10}Be in loess. Science ***360***, 877–881.
100. Cai, Y.J., An, Z.S., Cheng, H., et al. (2006). High-resolution absolute-dated Indian Monsoon record between 53 and 36 ka from Xiaobailong Cave, southwestern China. Geol. ***34***, 621–624.
101. Rohling, E.J., Liu, Q.S., Roberts, A.P., et al. (2009). Controls on the East Asian monsoon during the last glacial cycle, based on comparison between Hulu Cave and polar ice-core records. Quat. Sci. Rev. ***28***, 3291–3302.
102. An, Z.S., Clemens, S.C., Shen, J., et al. (2011). Glacial-interglacial Indian summer monsoon dynamics. Science ***333***, 719–723.
103. Wen, Q., Liu, Z., Zhu, J., et al. (2022). Local insolation drives Afro-Asian monsoon at orbital-scale in Holocene. Geophys. Res. Lett. ***49***, e2021GL097661. https://doi.org/10.1029/2021GL097661.
104. Ding, Y.H., Li, C.Y., and Liu, Y.J. (2004). Overview of the south China sea monsoon experiment. Adv. Atmos. Sci. ***21***, 343–360.
105. Tang, X., Qian, W.H., and Liang, P. (2006). Climate features of boundary belt for East Asian summer monsoon (in Chinese). Plateau Meteorol. ***25***, 375–381.
106. Rosenthal, Y., Oppo, D.W., and Linsley, B.K. (2003). The amplitude and phasing of climate change during the last deglaciation in the Sulu Sea, western equatorial Pacific. Geophys. Res. Lett. ***30***, 1428.

107. Oppo, D.W., and Sun, Y. (2005). Amplitude and timing of sea-surface temperature change in the northern South China Sea: dynamic link to the East Asian monsoon. Geol. ***33***, 785–788.
108. Bolliet, T., Holbourn, A., Kuhnt, W., et al. (2011). Mindanao dome variability over the last 160 kyr: episodic glacial cooling of the west pacific warm pool. Paleoceanography ***26***, PA1208.
109. Jian, Z.M., Wang, Y., Dang, H.W., et al. (2020). Half-precessional cycle of thermocline temperature in the western equatorial Pacific and its bihemispheric dynamics. Proc. Natl. Acad. Sci. USA ***117***, 7044–7051.
110. De Garidel-Thoron, T., Rosenthal, Y., Bassinot, F., and Beaufort, L. (2005). Stable sea surface temperatures in the western Pacific warm pool over the past 1.75 million years. Nature ***433***, 294–298.
111. Saraswat, R., Singh, D.P., Lea, D.W., et al. (2019). Indonesian throughflow controlled the westward extent of the Indo-Pacific Warm Pool during glacial-interglacial intervals. Glob. Planet. Change ***183***, 103031.
112. Gebregiorgis, D., Hathorne, E.C., Giosan, L., et al. (2018). Southern Hemisphere forcing of South Asian monsoon precipitation over the past ∼1 million years. Nat. Commun. ***9***, 4702.
113. Schmidt, G.A., LeGrande, A.N., and Hoffmann, G. (2007). Water isotope expressions of intrinsic and forced variability in a coupled ocean-atmosphere model. J. Geophys. Res. ***112***, 1–18.
114. Braconnot, P., Marzin, C., Grégoire, L., et al. (2008). Monsoon response to changes in Earth's orbital parameters: comparisons between simulations of the Eemian and of the Holocene. Clim. Past ***4***, 281–294.
115. Battisti, D.S., Ding, Q., and Roe, G.H. (2014). Coherent pan-Asian climatic and isotopic response to orbital forcing of tropical insolation. J. Geophys. Res. Atmos. ***119***, 11997–12020.
116. Liu, Z.Y., Wen, X.Y., Brady, E.C., et al. (2014). Chinese cave records and the East Asia summer monsoon. Quat. Sci. Rev. ***83***, 115–128.
117. Chiang, J.C., Fung, I.Y., Wu, C.H., et al. (2015). Role of seasonal transitions and westerly jets in East Asian paleoclimate. Quat. Sci. Rev. ***108***, 111–129.
118. Kong, W., Swenson, L.M., and Chiang, J.C.H. (2017). Seasonal transitions and the westerly jet in the Holocene East Asian summer monsoon. J. Clim. ***30***, 3343–3365.
119. Tabor, C.R., Otto-Bliesner, B.L., Brady, E.C., et al. (2018). Interpreting precession-driven $\delta^{18}O$ variability in the South Asian monsoon region. J. Geophys. Res. Atmos. ***123***, 5927–5946.
120. Lee, J., Fox-Kemper, B., Horvat, C., and Ming, Y. (2019). The response of East Asian monsoon to the precessional cycle: a new study using the geophysical fluid dynamics laboratory model. Geophys. Res. Lett. ***46***, 11388–11396.
121. Huang, E.Q., Zhao, M., Wang, Y., et al. (2020). Quaternary precession cycles of sea-surface oxygen isotope records from the tropical western pacific (in Chinese). Quat. Sci. ***40***, 1464–1473.
122. Clemens, S.C., and Prell, W.L. (1990). Late Pleistocene variability of Arabian Sea summer monsoon winds and continental aridity: eolian records from the lithogenic component of deep-sea sediments. Paleoceanography ***5***, 109–145.
123. Caley, T., Malaizé, B., Zaragosi, S., et al. (2011). New Arabian Sea records help decipher orbital timing of Indo-Asian monsoon. Earth Planet Sci. Lett. ***308***, 433–444.
124. Caley, T., Roche, D.M., and Renssen, H. (2014). Orbital Asian summer monsoon dynamics revealed using an isotope-enabled global climate model. Nat. Commun. ***5***, 5371. https://doi.org/10.1038/ncomms6371.
125. Bolton, C.T., Chang, L., Clemens, S.C., et al. (2013). A 500, 000 year record of Indian summer monsoon dynamics recorded by eastern equatorial Indian Ocean upper water-column structure. Quat. Sci. Rev. ***77***, 167–180.
126. Cronin, M.F., and McPhaden, M.J. (1998). Upper ocean salinity balance in the western equatorial Pacific. J. Geophys. Res. ***103***, 27567–27587.
127. Gebregiorgis, D., Clemens, S., Hathorne, E., et al. (2020). A brief commentary on the interpretation of Chinese speleothem $\delta^{18}O$ records as summer monsoon intensity tracers. Quaternary ***3***, 7. https://doi.org/10.3390/quat3010007.
128. Clemens, S.C., Prell, W.L., Sun, Y., et al. (2008). Southern hemisphere forcing of pliocene $\delta^{18}O$ and the evolution of indo-asian monsoons. Paleoceanography ***23***, PA4210.
129. Clemens, S.C., Prell, W.L., and Sun, Y. (2010). Orbital-scale timing and mechanisms driving Late Pleistocene Indo-Asian summer monsoons: reinterpreting cave speleothem $\delta^{18}O$. Paleoceanography ***25***, PA4207.
130. Zhao, D., Wan, S., Lu, Z., et al. (2020). Response of heterogeneous rainfall variability in East Asia to Hadley circulation reorganization during the late quaternary. Quat. Sci. Rev. ***247***, 106562.
131. Zhang, H.W., Cheng, H., Baker, J., and Kathayat, G. (2020). Response to Comments by Daniel Gebregiorgis et al. "A Brief Commentary on the Interpretation of Chinese Speleothem $\delta^{18}O$ Records as Summer Monsoon Intensity Tracers". Quaternary ***3***, 8.
132. Jalihal, C., Srinivasan, J., and Chakraborty, A. (2019). Modulation of Indian monsoon by water vapor and cloud feedback over the past 22, 000 years. Nat. Commun. ***10***, 5701–5708.
133. Zhang, H., Zhang, X., Cai, Y., et al. (2021). A data-model comparison pinpoints Holocene spatiotemporal pattern of East Asian summer monsoon. Quat. Sci. Rev. ***261***, 106911.
134. Jalihal, C., Srinivasan, J., and Chakraborty, A. (2022). Response of the low-level jet to precession and its implications for proxies of the Indian monsoon. Geophys. Res. Lett. ***49***, e2021GL094760.
135. An, Z.S., and Sun, D.H. (1995). Discussion on the monsoon variation over the Loess Plateau in the last glacial cycle. In China Contribution to Global Change, D.Z. Ye and H. Lin, eds. (Beijing Science Press), pp. 154–157.
136. Guo, B.H., Nie, J.S., Stevens, et al. (2022). Dominant Precessional Forcing of the East Asian Summer Monsoon since 260 Ka. Geology.
137. Zhao, Y., and Harrison, S.P. (2012). Mid-Holocene monsoons: a multi-model analysis of the inter-hemispheric differences in the responses to orbital forcing and ocean feedbacks. Clim. Dyn. ***39***, 1457–1487.
138. Nie, J.S., King, J.W., and Fang, X.M. (2008). Tibetan uplift intensified the 400 k.y. signal in paleoclimate records at 4Ma. Geol. Soc. Am. Bull. ***120***, 1338–1344.
139. Liu, C., Nie, J., Li, Z., et al. (2021). Eccentricity forcing of East Asian monsoonal systems over the past 3 million years. Proc. Natl. Acad. Sci. USA ***118***, e2107055118.
140. Windler, G., Tierney, J.E., and Anchukaitis, K.J. (2021). Glacial-interglacial shifts dominate tropical Indo-Pacific hydroclimate during the late Pleistocene. Geophys. Res. Lett. ***48***, e2021GL093339.
141. Shi, Z.G., Xie, X., Ren, X., et al. (2019). Radiative effect of mineral dust on east Asian summer monsoon during the Last Glacial Maximum: role of snow-albedo feedback. Geophys. Res. Lett. ***46***, 10901–10909.
142. Yi, L., Shi, Z.G., Tan, L., and Deng, C. (2018). Orbital-scale nonlinear response of East Asian summer monsoon to its potential driving forces in the late Quaternary. Clim. Dyn. ***50***, 2183–2197.
143. Bereiter, B., Eggleston, S., Schmitt, J., et al. (2015). Revision of the EPICA Dome C CO_2 record from 800 to 600 kyr before present. Geophys. Res. Lett. ***42***, 542–549.
144. Shakun, J.D., Lea, D.W., Lisiecki, L.E., and Raymo, M.E. (2015). An 800-kyr record of global surface ocean $\delta^{18}O$ and implications for ice volume-temperature coupling. Earth Planet Sci. Lett. ***426***, 58–68.
145. Chen, S.T., Wang, Y.J., Cheng, H., et al. (2016). Strong coupling of Asian Monsoon and Antarctic climates on sub-orbital timescales. Sci. Rep. ***6***, 32995.
146. Sigman, D.M., Hain, M.P., and Haug, G.H. (2010). The polar ocean and glacial cycles in atmospheric CO_2 concentration. Nature ***466***, 47–55.
147. Veres, D., Bazin, L., Landais, A., et al. (2013). The Antarctic ice core chronology (AICC2012): an optimized multi-parameter and multi-site dating approach for the last 120 thousand years. Clim. Past ***9***, 1733–1748.
148. Loulergue, L., Schilt, A., Spahni, R., et al. (2008). Orbital and millennial-scale features of atmospheric CH_4 over the past 800, 000 years. Nature ***453***, 383–386.
149. Cheng, H., Zhang, H.W., Spötl, C., et al. (2020). Timing and structure of the Younger Dryas event and its underlying climate dynamics. Proc. Natl. Acad. Sci. USA ***117***, 23408–23417.
150. Cheng, H., Xu, Y., Dong, X.Y., et al. (2021). Onset and termination of Heinrich Stadial 4 and the underlying climate dynamics. Commun. Earth Environ. ***2***, 230–311.
151. Marcott, S.A., Bauska, T.K., Buizert, C., et al. (2014). Centennial-scale changes in the global carbon cycle during the last deglaciation. Nature ***514***, 616–619.
152. Böhm, E., Lippold, J., Gutjahr, M., et al. (2015). Strong and deep Atlantic meridional overturning circulation during the last glacial cycle. Nature ***517***, 73–76.
153. Henry, L.G., McManus, J.F., Curry, W.B., et al. (2016). North Atlantic Ocean circulation and abrupt climate change during the last glaciation. Science ***353***, 470–474.
154. Bauska, T.K., Marcott, S.A., Brook, E.J., et al. (2021). Abrupt changes in the global carbon cycle during the last glacial period. Nat. Geosci. ***14***, 91–96.
155. Stríkis, N.M., Chiessi, C.M., Cruz, F.W., et al. (2015). Timing and structure of mega-SACZ events during Heinrich stadial 1. Geophys. Res. Lett. ***42***, 5477–5484A.
156. Zhang, X., Knorr, G., Lohmann, G., and Barker, S. (2017). Abrupt North Atlantic circulation changes in response to gradual CO_2 forcing in a glacial climate state. Nat. Geosci. ***10***, 518–523.
157. Roberts, N.L., Piotrowski, A.M., McManus, J.F., and Keigwin, L.D. (2010). Synchronous deglacial overturning and water mass source changes. Science ***327***, 75–78.
158. Deaney, E.L., Barker, S., van de Flierdt, T., et al. (2017). Timing and nature of AMOC recovery across Termination 2 and magnitude of deglacial CO_2 change. Nat. Commun. ***8***, 14595.
159. Roche, D.M., Wiersma, A.P., and Renssen, H. (2010). A systematic study of the impact of freshwater pulses with respect to different geo- graphical locations. Clim. Dyn. ***34***, 997–1013.
160. Yin, Q.Z., Wu, Z.P., Berger, A., et al. (2021). Insolation triggered abrupt weakening of Atlantic circulation at the end of interglacials. Science ***373***, 1035–1040.
161. Dong, X.Y., Kathayat, G., Rasmussen, S.O., et al. (2022). Coupled atmosphere-ice-ocean dynamics during Heinrich Stadial 2. Nat. Commun. ***13***, 5867.
162. Broecker, W.S. (1991). The Great Ocean Conveyor (Princeton Univ. Press).
163. Burckel, P., Waelbroeck, C., Luo, Y., et al. (2016). Changes in the geometry and strength of the Atlantic meridional overturning circulation during the last glacial (20–50 ka). Clim. Past ***12***, 2061–2075.
164. Krebs, U., and Timmermann, A. (2007). Tropical air–sea interactions accelerate the recovery of the atlantic meridional overturning circulation after a major shutdown. J. Clim. ***20***, 4940–4956.
165. Jahfer, S., Vinayachandran, P.N., and Nanjundiah, R.S. (2020). The role of Amazon River runoff on the multidecadal variability of the Atlantic ITCZ. Environ. Res. Lett. ***15***, 054013.
166. Liang, Y.C., Lo, M.H., Lan, C.W., et al. (2020). Amplified seasonal cycle in hydroclimate over the Amazon River basin and its plume region. Nat. Commun. ***11***, 4390.
167. Masson, S., and Delecluse, P. (2001). Influence of the Amazon River runoff on the tropical atlantic. Phys. Chem. Earth - Part B Hydrol., Oceans Atmos. ***26***, 137–142.

168. Pedro, J.B., Jochum, M., Buizert, C., et al. (2018). Beyond the bipolar seesaw: toward a process understanding of interhemispheric coupling. Quat. Sci. Rev. ***192***, 27–46.
169. Adhémar, J.A. (1842). Revolutions of the Sea (In French) (Carilian-Goeury et V. Dalmont).
170. Croll, J. (1875). Climate and Time in Their Geological Relations: A Theory of Secular Changes of the Earth's Climate (Daldy Isbister, & Co.).
171. Lu, Z.Y., Liu, Z.Y., Chen, G.S., and Guan, J. (2019). Prominent precession band variance in ENSO intensity over the last 300, 000 years. Geophys. Res. Lett. ***46***, 9786–9795.

ACKNOWLEDGMENTS

This work was supported by the National Natural Science Foundation of China (41888101 and 42150710534).

AUTHOR CONTRIBUTIONS

H.C. wrote the draft manuscript. A.S., Q.Y., Z.S., Y.C., Y.H., Q.H., and J.T. revised the manuscript. H.L., L.S., X.D., J.Z., Z.L., and Z.S. performed data analyses and simulations. All authors reviewed and provided revisions for the manuscript.

DECLARATION OF INTERESTS

The authors declare no competing interests.

LEAD CONTACT WEBSITE

https://gr.xjtu.edu.cn/web/cheng021/home.